Dalton Transactions

ROYAL SOCIETY OF CHEMISTRY

PAPER

View Article Online
View Journal

Open Access Article. Published on 04 December 2025. Downloaded on 12/24/2025 9:36:28 PM.
This article is licensed under a Creative Commons Attribution-NonCommercial 3.0 Unported Licence.

Check for updates

Cite this: DOI: 10.1039/d5dt01792k

Palladium(0) and Juglone: a new alliance in the fight against ovarian cancer

Giovanni Tonon,[a] Anna Rafaniello,[a] Matteo Mauceri,[a] Nicola Demitri,[b] Thomas Scattolin,*[c] Flavio Rizzolio*[a,d] and Fabiano Visentin*[a]

Multitarget drugs represent one of the most appropriate responses to a multifaceted and elusive disease such as cancer. Besides, the option of introducing more active substances in a single compound may prove beneficial to simplify the administration of the drug and improve its pharmacokinetics. Here, the synthesis of a new class of palladium(0) complexes coordinating one molecule of Juglone has been developed, optimizing a versatile method that allows to easily select the kind of ancillary ligands, including phosphines, arsines, isocyanides, and N-heterocyclic carbenes. All the newly synthesised metal compounds have been fully characterized by spectroscopic methods and, in some cases, by X-ray diffractometry. Juglone is a natural-source organic compound derived from many species of the *Juglandaceae* family, whose therapeutic properties have long been known. In particular, its inhibitory activity toward PIN1—a fast-acting enzyme upregulated in cells and tissues of various neoplasms, especially ovarian cancer—can be exploited to reduce tumor proliferation. On the other hand, some of our previous works have shown the antiproliferative activity of different palladium(0) derivatives, in particular towards ovarian cancer cells. In this work, we prove that the η^2-coordination of Juglone on the palladium(0) center can, in some cases, amplify its *in vitro* anticancer activity towards different ovarian cancer cell lines, probably by leveraging the combined effect of the natural organic molecule and the metal residue. A further added value is represented by the reduced cytotoxicity exhibited by most of our palladium complexes against MRC-5 non-cancerous cells (IC_{50} > 100 μM). At the same time, our synthesized complexes maintain high effectiveness against cisplatin-resistant and high-grade serous ovarian cancer cell lines, with IC_{50} values in the micromolar range. Finally, western blot analysis carried out on one of the most active complexes has proven its high inhibitory effect on the PIN1 oncogenic protein.

Received 28th July 2025,
Accepted 3rd December 2025

DOI: 10.1039/d5dt01792k

rsc.li/dalton

Introduction

Cancer is a complex disease and therefore demands equally complex therapeutic strategies.[1–4] The notion that a single kind of treatment can prove decisive in definitively defeating this pathology appears to have waned. Consequently, many therapeutic protocols employ a well-calibrated combination of multiple approaches (surgical, chemotherapeutic, radiotherapeutic, immunotherapeutic, and hormonal) tailored to the specific forms of neoplasia and possibly to the individual characteristics of each patient.[5–7]

Even within the more restricted framework of chemotherapy, a multifaceted strategy is commonly adopted, and the use of drug cocktails targeting distinct molecular pathways and modes of action has become a well-established clinical practice.[8]

An important step forward in this direction is represented by the integration of more than one active principle in a single compound. Formulating a single drug that contains multiple active ingredients offers considerable advantages from the pharmacokinetic point of view, as well as making its administration easier.

Transition-metal complexes seem well suited for this purpose, as their coordination sites can be exploited to bind different pharmacologically active molecules. Moreover, the metal centre itself exhibits intrinsic cytotoxicity, thereby contributing to the overall therapeutic action of the drug and potentially promoting a synergistic effect.[9–11]

Promising results in this area have been achieved by employing inert Pt(IV) octahedral complexes as prodrugs, which are reduced within the tumour environment to square-planar Pt(II) complexes (typically cisplatin), accompanied by the concurrent release of bioactive molecules coordinated at axial positions.[12–15]

[a]Dipartimento di Scienze Molecolari e Nanosistemi, Università Ca' Foscari, Campus Scientifico Via Torino 155, 30174 Venezia-Mestre, Italy. E-mail: fvise@unive.it
[b]Elettra – Sincrotrone Trieste, S.S. 14 Km 163.5 in Area Science Park, 34149 Basovizza, Trieste, Italy
[c]Dipartimento di Scienze Chimiche, Università degli Studi di Padova, via Marzolo 1, 35131 Padova, Italy. E-mail: thomas.scattolin@unipd.it
[d]Pathology Unit, Centro di Riferimento Oncologico di Aviano (C.R.O.) IRCCS, via Franco Gallini 2, 33081 Aviano, Italy. E-mail: flavio.rizzolio@unive.it

Open Access Article. Published on 04 December 2025. Downloaded on 12/24/2025 9:36:28 PM.
This article is licensed under a Creative Commons Attribution-NonCommercial 3.0 Unported Licence.

Although cisplatin and its second- and third-generation derivatives have marked a pivotal turning point in chemotherapy based on metallodrugs and still play a leading role in many therapeutic protocols,[16–18] researchers are gradually directing their efforts towards alternative transition-metal derivatives in an attempt to reduce the numerous drawbacks of platinum compounds.

In recent years, palladium complexes have been gaining ground in this field,[19,20] owing to the close similarity in coordination chemistry between this metal and platinum. Most reports have focused on Pd(II) complexes, where the inherently fast ligand-exchange rates compared to platinum analogues are generally mitigated through the use of strongly coordinating ligands, which are able to guarantee sufficient stability in the bloodstream and cellular environment.[21–26]

Several palladium complexes have shown promising anticancer activity, often comparable to (or even surpassing) that of cisplatin, and occasionally combine this high cytotoxicity against diverse cancer cell lines with a reduced effect on non-tumour cells.[19,27,28] This proved to be especially true for organopalladium compounds, to which our research group has devoted particular attention in recent years, synthesizing a wide range of compounds and demonstrating their antiproliferative properties mainly towards ovarian cancer cells.[28–34]

Moreover, the mechanism of action of these compounds appears in many cases to differ from that of classical platinum-based drugs, suggesting their potential use in the treatment of cisplatin-resistant forms of ovarian cancer.

Much less information is available on the anticancer properties of palladium(0) derivatives, which are relatively rare and typically less stable than the more extensively studied palladium(II) species.[35–38]

A class of palladium(0) compounds sufficiently stable to operate under biological conditions includes species of the type [Pd(L^L′)(η^2-olefin)] or [PdLL′(η^2-olefin)], provided that the olefin bears electron-withdrawing substituents and bidentate L^L′ or monodentate L/L′ ligands exhibit strong coordinating capability. Typically, ligands such as P-donor phosphines, N-donor pyridines or quinolines, S-donor thiols, and C-donor N-heterocyclic carbenes are employed; in some cases, the bidentate ligands are heteroditopic.[39,40]

Juglone is an olefin with high π-electron-acceptor character and can effectively coordinate to the electron-rich palladium(0) centre, thereby taking advantage of strong metal–ligand π-back-bonding. In addition, it is a natural compound found mainly in several species of the *Juglandaceae* family, which has become a subject of increasing interest in medicinal research for its antifungal,[41] antibacterial,[42] antiviral,[43] and anti-inflammatory[44] properties.

Numerous studies have demonstrated that this compound efficiently inhibits the growth of *Staphylococcus aureus*,[45] *Escherichia coli*[46] and *Candida albicans*,[47] through a mechanism involving the disruption of bacterial and fungal cell membranes, ultimately leading to cell death.

More recent works have also investigated the inhibitory effects of Juglone against various viruses, including herpes simplex virus (HSV) and influenza.[48] The anti-inflammatory properties of Juglone stem from its ability to inhibit pro-inflammatory cytokines such as TNF-α, IL-6, and IL-1β, making it a promising candidate for the treatment of inflammatory diseases such as arthritis and inflammatory bowel disease (IBD).[49]

Finally, Juglone has been successfully evaluated as an anticancer agent, proving its ability to induce apoptosis in various cancer cell lines including breast, lung, and colon cancer. In these cases, its mechanism of action seems to involve the generation of reactive oxygen species (ROS), resulting in mitochondrial dysfunction and cell-cycle arrest.[50,51] Interestingly, several studies have proven that Juglone is a potent PIN1 inhibitor, a fast-acting enzyme upregulated in cells and tissues of certain kinds of neoplasia such as prostate cancer, glioblastoma and, above all, ovarian cancer. PIN1 downregulates apoptotic signals by targeting serine/threonine-proline motifs, thereby facilitating cell proliferation.[52–55]

In this work, we report for the first time a system featuring a palladium(0) centre incorporating Juglone, with the main objective of assessing whether the cytotoxicity of Juglone toward ovarian cancer cells can be enhanced through its coordination to a palladium(0) metal centre (Fig. 1).

This hypothesis stems from our previous findings, which demonstrated that palladium(0) complexes are capable of exerting a remarkable antitumor effect that could act synergistically with that of Juglone. Furthermore, the influence of different ancillary ligands (L^L′ or L/L′)—including aromatic phosphines, arsines, isocyanides, and N-heterocyclic carbenes—on the anticancer activity of the synthesized [Pd(L^L′)(η^2-Juglone)] and [PdLL′(η^2-Juglone)] complexes (Scheme 1) was evaluated. Finally, the inhibition of PIN1 by a model Juglone–Pd(0) complex was investigated in detail.

Results and discussion

Synthetic routes to Pd(0)-η^2-Juglone complexes

In order to establish the best strategy to prepare Pd(0)-η^2-Juglone complexes bearing different mono- or bidentate phosphines as ancillary ligands, three different synthetic approaches were preliminarily explored.

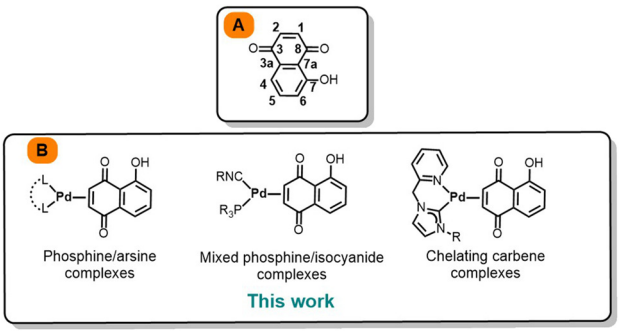

Fig. 1 (A) Juglone structure. (B) Pd(0)-Juglone complexes synthesized in this work.

Open Access Article. Published on 04 December 2025. Downloaded on 12/24/2025 9:36:28 PM.
This article is licensed under a Creative Commons Attribution-NonCommercial 3.0 Unported Licence.

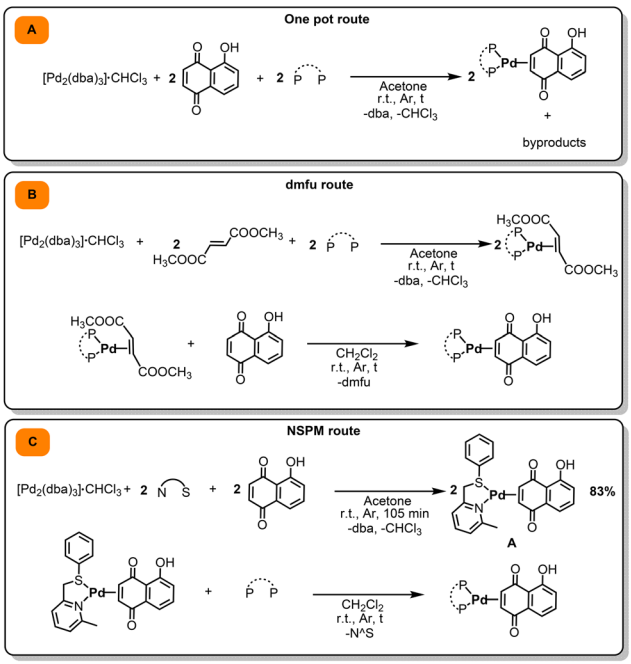

Scheme 1 Synthetic routes to target complexes. (A) One-pot route. (B) dmfu route. (C) NSPM route used in this work.

The first option is represented by the most direct one-pot procedure, consisting of mixing in the reaction vessel the metal precursor $[Pd_2(dba)_3{\cdot}CHCl_3]$ (dba = dibenzylideneacetone), Juglone, and the chosen phosphine (Scheme 1A). This method, carried out in anhydrous acetone at room temperature, had already been successfully adopted in the past by our research group to prepare complexes of the type $[Pd(P^\wedge P)(\eta^2\text{-olefin})]$ or $[Pd(PR_3)_2(\eta^2\text{-olefin})]$ with a large library of electron-withdrawing olefins and ancillary ligands.[56–59] Unfortunately, in this case the outcome was not as expected, yielding in the final mixture, in addition to the desired product, small but significant amounts of by-products, which were difficult to separate and identify.

Assuming that the formation of by-products was caused by the simultaneous presence in the reaction mixture of Juglone and phosphines, we planned to prepare the target complexes adopting a two-step procedure, in order to keep the two reagents separated (Scheme 1B). In the first step, we synthesized complexes of the type $[Pd(P^\wedge P)(\eta^2\text{-dmfu})]$ or $[Pd(PR_3)_2(\eta^2\text{-dmfu})]$ (dmfu = dimethyl fumarate) starting from $[Pd_2(dba)_3{\cdot}CHCl_3]$ and dmfu. In this case, a reaction time of 90 minutes at room temperature was sufficient to ensure the complete formation of the Pd(0)-dmfu complex, which was smoothly isolated after an appropriate work-up. In the second step, it was possible to take advantage of the lability of dmfu, which can be removed from the palladium(0) centre and replaced by Juglone. In this context, in our previous works we have proven that 1,4-naphthoquinone binds to the palladium (0) centre much more firmly than dmfu;[56] we estimated the equilibrium constant for the substitution of dmfu with 1,4-naphthoquinone in $[Pd(L^\wedge L)(\eta^2\text{-dmfu})]/[Pd(L)_2(\eta^2\text{-dmfu})]$ complexes to be about 1×10^3, regardless of the nature of the L^L/L ancillary ligand. Given the close resemblance of Juglone to 1,4-naphthoquinone, we verified that only a slight excess of the former is sufficient to obtain the target complexes $[Pd(P^\wedge P)(\eta^2\text{-Juglone})]/[Pd(PR_3)_2(\eta^2\text{-Juglone})]$ from $[Pd(P^\wedge P)(\eta^2\text{-dmfu})]/[Pd(PR_3)_2(\eta^2\text{-dmfu})]$, which can be separated by precipitation with diethyl ether.

The synthetic strategy described above, although effective, nevertheless requires the preparation of a different intermediate product $[Pd(L^\wedge L)(\eta^2\text{-dmfu})]/[Pd(L)_2(\eta^2\text{-dmfu})]$ for each selected ligand L or L^L.

To streamline the procedure, we attempted to synthesize the complex $[Pd(NSPM)(\eta^2\text{-Juglone})]$, where NSPM = 2-methyl-6-((phenylthiol)methyl)pyridine (Scheme 1C). Our intention was to exploit the lability of the pyridyl-thioether NSPM ligand, which arises from the distortion of the chelate ring mainly induced by the presence of an *ortho*-methyl substituent on the pyridine ring.[60,61] In this way, starting from a single intermediate species it is possible to prepare all target complexes simply by substituting NSPM with the selected monodentate or bidentate phosphine ligand.

The synthesis of $[Pd(NSPM)(\eta^2\text{-Juglone})]$ complex, carried out in acetone at room temperature by mixing $[Pd_2(dba)_3{\cdot}CHCl_3]$, Juglone, and NSPM, was successful. The final palladium(0) complex was isolated by washing the residue obtained after removal of the solvent from the reaction mixture with diethyl ether and *n*-pentane. The identity of this product can be ascertained by the analysis of its NMR spectra. It is important to point out that the mutual orientation of the NSPM ligand and Juglone (both unsymmetrical molecules) can potentially generate four different positional isomers. However, the ^{1}H NMR spectrum, recorded at room temperature, appears relatively simple and seems to indicate the presence of a single specie. Actually, the fact that some peaks appear slightly broadened suggests a fluxional behaviour of the complex, which promotes a rapid interconversion of the isomers.

Upon lowering the temperature to 223 K (Fig. S2 in SI), a partial splitting of several signals was observed, particularly those associated with the diagnostic OH resonance between 12.5 and 14 ppm; however, complete freezing of all fluxional processes was not achieved.

This kind of phenomenon has been thoroughly examined by our research group in the past for similar systems and can be attributed to the rapid inversion of configuration at the coordinated sulphur and/or pseudo-rotation of the olefin.[56]

In any case, the coordination of Juglone in the isolated product is unambiguously attested by the presence, in its ^{1}H NMR spectrum, of a broad singlet at 4.89 ppm assignable to the two olefinic protons of Juglone, which resonate at chemical shifts significantly lower than those of the uncoordinated molecule. This effect is well known and is a direct consequence of strong palladium–olefin π-back bonding. A resonance at 13.15 ppm corresponds to the OH group. On the other hand, the coordination of the NSPM ligand is confirmed

Open Access Article. Published on 04 December 2025. Downloaded on 12/24/2025 9:36:28 PM.
This article is licensed under a Creative Commons Attribution-NonCommercial 3.0 Unported Licence.

by the signals of CH_2S and CH_3 groups, resonating at 4.83 and 2.82 ppm, respectively. Finally, in the region of the spectrum between 6.98 and 7.24 ppm, all the aromatic proton signals of both NSPM and Juglone are observed.

Synthesis of complexes bearing bidentate phosphines and arsines

Our final choice for preparing the target complexes, as well as those described in the following paragraphs, was to adopt as a universal precursor the complex [Pd(NSPM)(η^2-Juglone)], subsequently replacing the pyridylthioether ligand with the selected bidentate phosphines/arsines. This exchange reaction was conducted in dichloromethane at room temperature, employing only a slight excess of the bidentate ligand. The separation of the final products from the reaction mixture was also straightforward, requiring only the treatment of the residue obtained after evaporation of the solvent with diethyl ether or diethyl ether/*n*-pentane, a procedure sufficient to remove the released NSPM ligand. All the synthesized complexes are reported in Scheme 2.

As is customary for the characterization of this class of complexes, NMR spectroscopy was employed. The $^{31}P\{^1H\}$ NMR spectra are all characterized by the presence of two doublets or an AB system, since the two phosphorus atoms of the bidentate ligand are made inequivalent by the dissymmetry of the coordinated Juglone.

The coordination of Juglone to the palladium centre is convincingly evidenced by the positions of the signals of the olefinic protons in the ^1H NMR spectra. These signals, which typically appear as an AA′XX′ system due to coupling with the phosphorus nuclei, always resonate between 4 and 5 ppm, namely at chemical shifts 2–3 ppm lower than those of the free olefin. This effect arises from significant Juglone-palladium π-backdonation. Remarkably, the signal of the Juglone hydroxyl proton is also observed in the spectra of these complexes at lower ppm values compared to the uncoordinated molecule.

The $^{13}C\{^1H\}$ NMR spectra provide further insights. In addition to confirming the major role of metal-olefin backdonation, which accounts for particularly low chemical shifts of the two olefinic carbons C1 and C2 (about 70 ppm lower than those of free Juglone), the peaks corresponding to the other carbons of Juglone can also be traced. In particular, the resonances of carbons C4, C6, and C7a generate three well-recognizable peaks in the spectra between 116 and 120 ppm. Moreover, it is always easy to locate the signals of the two carbonyl carbons C8 and C3 (at 180–190 ppm) and that of carbon C7, bound to the hydroxyl group, around 160 ppm.

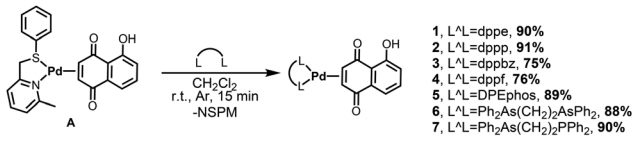

Scheme 2 Synthesis of Pd(0)-η^2-Juglone complexes with bidentate phosphines and arsines.

Particular attention should be paid to complex [Pd($Ph_2AsCH_2CH_2PPh_2$)(η^2-Juglone)] (**7**), which features a ligand containing two different donor atoms (As and P). In fact, this asymmetry, combined with that of Juglone, leads to the formation of two different isomers that, being structurally very similar, are present in comparable amounts.

This is evidenced by the $^{31}P\{^1H\}$ NMR spectrum which displays two signals of equal intensity at approximately 43 ppm.

Consistently, the ^1H NMR spectrum is characterized by the signals of two different species, among which those due to the OH group are particularly diagnostic. They are located at 13.21 and 13.41 ppm, respectively, and show essentially the same integration. Notably, the signals of the olefinic protons are partially overlapped, at approximately 5.3 ppm.

Conversely, in the $^{13}C\{^1H\}$ NMR spectrum, the olefinic carbons of the two isomers are well distinguished, with the C1 carbons (*trans* to the phosphorus donor atom) resonating as two doublets ($J_{P-C} \approx 18$ Hz) between 68 and 69 ppm, whereas the C2 carbons (*trans* to arsenic) appear as closer doublets ($J_{P-C} \approx 2$ Hz) between 69.5 and 70.5 ppm. A similar trend is observed for the carbonyl carbons, which appear as doublets ($J_{P-C} \approx 7.1$ Hz) when *trans* to phosphorus (C8) and singlets when *trans* to arsenic (C3). These signals are located at 188–189 ppm.

Due to their close similarity in polarity and solubility, the two isomers cannot be separated and therefore will be biologically tested as a mixture.

The characterization of all these new complexes was also complemented with IR spectra, in which the C═O stretching band of the Juglone carbonyl groups is particularly intense and diagnostic. In general, there is a significant lowering of the frequency of this signal compared to the free olefin (approximately 40 cm^{-1}).

Finally, definitive proof of the nature of the synthesized complexes is provided by the determination of the solid-state structure of two of them, namely [Pd(DPEPhos)(η^2-Juglone)] (**5**) and [Pd($Ph_2AsCH_2CH_2PPh_2$)(η^2-Juglone)] (**7**) (only one of the two isomers), obtained by single-crystal X-ray analysis (see Fig. 2 and Tables S2, S3, S4). Crystals were obtained by slow diffusion of diethyl ether in a dichloromethane solution of complexes **5** and **7**.

Notably, the Pd–C1, Pd–C2, and C1–C2 bond lengths, which directly or indirectly reflect the bond strength between the Juglone ligand and the metal centre, are consistent with the values reported in the literature.[39]

Synthesis of complexes bearing monodentate phosphines and arsines

Taking advantage of the synthetic approach described in the previous section, we were able to prepare the Pd(0)–η^2-Juglone derivatives bearing monodentate aryl phosphines as ancillary ligands.

Our plan was to investigate whether the nature of the *para*-substituent X (X = H, F, Cl, OMe) of the employed aryl phos-

Open Access Article. Published on 04 December 2025. Downloaded on 12/24/2025 9:36:28 PM.
This article is licensed under a Creative Commons Attribution-NonCommercial 3.0 Unported Licence.

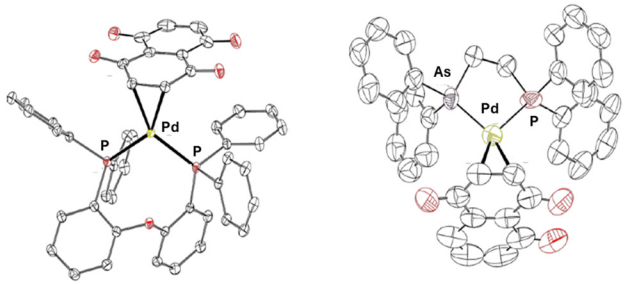

Fig. 2 X-ray molecular structures of **5** (left) and **7** (right) are presented, showing thermal displacement ellipsoids at the 50% probability level with hydrogen atoms and solvent molecules omitted for clarity.

phines could influence the cytotoxicity of the corresponding palladium(0) complexes. For the sake of completeness, we also synthesized the complex [Pd($AsPh_3$)$_2$(η^2-Juglone)] with the aim of evaluating the effect of the ligand donor atom as well.

To this end, starting from the common precursor [Pd(NSPM)(η^2-Juglone)], the addition of two equivalents of the selected phosphine/arsine allowed complete substitution of NSPM, and the final products were obtained after removal of the solvent (dichloromethane) and treatment of the residue with a mixture of diethyl ether and *n*-pentane (Scheme 3).

The identity of the complexes was first confirmed by the analysis of their NMR spectra. As expected, the $^{31}P\{^1H\}$ NMR spectra display an AB system because of the presence of two inequivalent phosphorus atoms in the complexes. The chemical shifts of the two signals are higher by 30–40 ppm compared to those of the corresponding free phosphine, thereby confirming the coordination of the ligand to the metal centre.

In the ^1H NMR spectra, the typical AA′XX′ system of the coordinated olefinic protons is detectable at approximately 4.6 ppm, whereas at the highest chemical shift (around 12.5 ppm) the singlet ascribable to the OH group can be identified. Finally, also in these cases, the high degree of Pd–Juglone backdonation lowers the chemical shift of the olefinic carbons to around 70 ppm and the C=O stretching frequency of the carbonyl groups to approximately 1600 cm^{-1}.

Synthesis of a complex bearing mixed isocyanide/phosphine ligands

A further option explored in this work involved the preparation of a Pd(0)-η^2-Juglone complex bearing two different ancillary ligands, namely an aryl phosphine and an alkyl isocyanide. This combination has previously proven particularly effective in enhancing the anticancer properties of other palladium organometallic derivatives previously synthesized by our group.[62]

As observed in similar contexts, the simultaneous addition of one equivalent each of phosphine and isocyanide to an appropriate Pd(0) precursor is sufficient to favour the formation of a mixed complex, at the expense of those containing either two phosphines or two isocyanides.[63]

Therefore, by mixing a dichloromethane solution of the [Pd(NSPM)(η^2-Juglone)] precursor with one containing one equivalent of triphenylphosphine and one equivalent of *tert*-butyl isocyanide, the desired product was obtained by following the same work-up procedure previously described (Scheme 4).

From the $^{31}P\{^1H\}$ NMR spectrum, it is immediately evident that the isolated product consists of a mixture of two isomers, which differ in the relative position of the isocyanide (or phosphine) ligand with respect to the OH group of Juglone. The two isomers must have similar thermodynamic stability, as their relative abundance is comparable (1 : 1.2).

This conclusion is supported by the proton spectrum, in which two distinct sets of signals can be distinguished. Among these, those of the OH and *tert*-butyl groups stand out around 13 and 1.2 ppm, respectively, whereas those of the olefinic protons are partially overlapped.

Accordingly, the $^{13}C\{^1H\}$ NMR signals are also divided into two groups. In particular, the two olefinic carbons of each isomer are easily distinguishable from each other: the carbons in *trans* position with respect to the phosphine appear as doublets (*ca.* 65 ppm, with J_{C-P} = 18.6 Hz), whereas those in *cis* position appear as singlets.

As in previous cases, separation of the two isomers by conventional methods proved to be practically impossible.

In the FT-IR spectrum of the complex, in addition to the strong absorption band of the C=O stretching around 1600 cm^{-1}, the intense C≡N stretching band of the *tert*-butyl isocyanide ligand can be detected at 2172 cm^{-1}. The increase in this frequency with respect to that of free *tert*-butyl isocyanide (2137 cm^{-1}) is a direct consequence of the coordination of the ligand to the Pd(0) centre.[64]

Gratifyingly, we were able to obtain the X-ray molecular structure of one of the two isomers, which is reported in Fig. 3.

Complex bearing a picolyl-functionalized N-heterocyclic carbene ligand

The last Pd(0)-η^2-Juglone complex prepared in this work is equipped with a picolyl-functionalized N-heterocyclic carbene ligand. This choice was motivated by the fact that the NHC–Pd bond is generally very strong and contributes to the overall

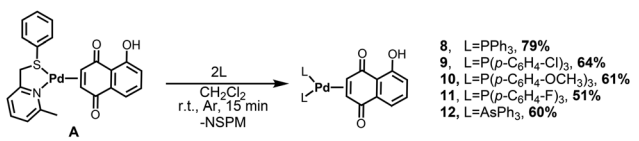

Scheme 3 Synthesis of Pd(0)-η^2-Juglone complexes with monodentate phosphines and arsines.

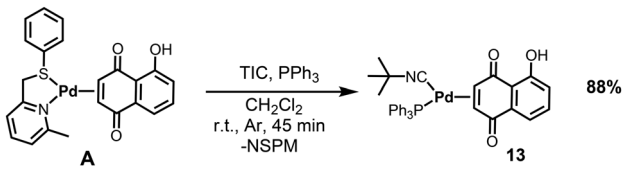

Scheme 4 Synthesis of mixed phosphine/isocyanide Pd(0)-η^2-Juglone complex **13**.

Open Access Article. Published on 04 December 2025. Downloaded on 12/24/2025 9:36:28 PM.
This article is licensed under a Creative Commons Attribution-NonCommercial 3.0 Unported Licence.

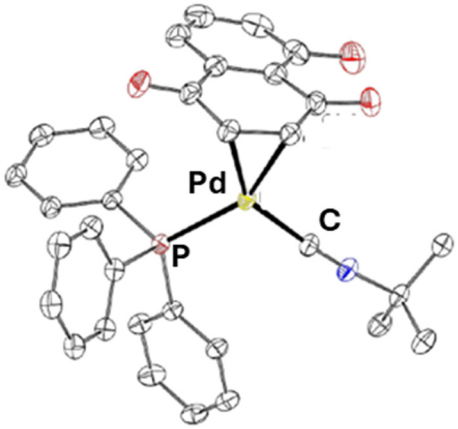

Fig. 3 X-ray molecular structures of complex **13** is presented, showing thermal displacement ellipsoids at the 50% probability level with hydrogen atoms and solvent molecules omitted for clarity.

stability of the complex, together with the chelating effect provided by the picolyl group. This, in turn, hampers decomposition processes that could compromise the biological activity of the complex.

The synthetic procedure adopted for the preparation of this complex involves a transmetalation reaction between [Pd(NSPM)(η^2-Juglone)] and the silver(I)–NHC complex **B**. This process enables the transfer of the picolyl-functionalized N-heterocyclic carbene from silver(I) to palladium(0), with the formation of insoluble silver bromide acting as the driving force of the reaction (Scheme 5).

Simple filtration of AgBr through a Celite pad, followed by solvent evaporation and treatment of the residual solid with diethyl ether, allows the isolation of the final product in good yield.

Also in this case, the dissymmetry of Juglone, combined with that of the NHC ligand, gives rise to two different isomers in an approximately 1 : 1 ratio. In fact, in the ^{1}H NMR spectrum, two sets of signals are clearly distinguishable, although they are sometimes partially overlapped. The signals related to the OH groups of the two isomers are well distinct, resonating at 13.04 and 14.64 ppm, whereas the signals attributable to the NCH_2 protons are not separable from each other and give rise to a complex multiplet at approximately 5.5 ppm. Conversely, the corresponding olefinic carbons are well distinguishable, with those in the *trans* position with respect to the carbene located between 65 and 68 ppm, and those in the *trans* position with respect to the pyridine between 57 and 59 ppm.

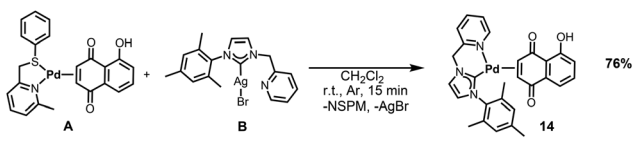

Scheme 5 Synthesis of [Pd(η^2-Juglone)] complex **14**.

The coordination of the picolyl-functionalized N-heterocyclic carbene can be confirmed by observing, in the $^{13}C\{^1H\}$ NMR spectrum, two peaks (one for each isomer) corresponding to the carbene carbon bound to the palladium (0) centre, located at 183.9 and 184.5 ppm, which give rise to two intense cross-peaks with the imidazole ring protons in the HMBC spectrum. Consistently, in the ^{1}H NMR spectrum, two doublets attributable to the *ortho* protons of the coordinated pyridine are observed at around 8.6 ppm. It should be noted that the interconversion between the two isomers is fast enough at room temperature that, in order to observe them as well-distinct signals, the NMR spectra must be recorded at least at 253 K.

Antiproliferative activity on ovarian cancer and normal cells

The entire library of novel Pd(0)-η^2-Juglone complexes was tested against a selection of ovarian cancer cell lines, including the classical A2780, its cisplatin-resistant counterpart A2780*cis*, OVCAR-5, and KURAMOCHI. The latter two are representative of high-grade serous ovarian cancer (HGSOC), the most aggressive form of this type of tumour. Moreover, the cytotoxicity of our metal derivatives was also evaluated against the non-cancerous MRC-5 (human lung fibroblast) cell line, in order to assess their potential selectivity of action. For comparison, the same tests were performed on the uncoordinated Juglone molecule and on the benchmark metal-based drug cisplatin, which therefore served as a positive control. As a preliminary step, the stability of the palladium(0) derivatives was evaluated in a 1 : 10 DMSO/H_2O solution containing 100 mM NaCl and 5 mM of the complex by NMR spectroscopy. Over a 48-hour period, no significant alterations were observed in the spectra, indicating that the complexes retained their structural integrity.

Furthermore, the stability of the complexes was evaluated in cell culture medium (DMEM/F12) by UV–Vis spectroscopy. Over a 24 h period, no significant changes were observed in the spectra, indicating that the complexes retained their structural integrity (Fig. S45–S47, SI). Cytotoxicity was assessed by determining IC_{50} values (half-maximal inhibitory concentrations), which are summarized in Table 1. Statistical analysis of the IC_{50} data is provided in the SI.

On the basis of these results, the following considerations can be proposed:

(a) Practically all complexes exhibit significant antiproliferative activity against the four ovarian cancer cell lines tested, with IC_{50} values in the micromolar or submicromolar range. Overall, these values are slightly higher than those of cisplatin for the A2780, OVCAR-5, and KURAMOCHI cell lines. The observed cytotoxicity is comparable to, or even higher than, that reported for related [Pd(PR_3)$_2$(η^2-olefin)] complexes in the literature.[35,39b] The only exceptions are represented by complexes **4** and **12** (bearing DPPF and two $AsPh_3$ ligands, respectively), whose cytotoxicity is markedly lower.

(b) Interestingly, almost all complexes display very low cytotoxicity (IC_{50} > 100 μM) towards non-cancerous MRC-5 cells. Even in the case of the two moderately active complexes **7** and

Open Access Article. Published on 04 December 2025. Downloaded on 12/24/2025 9:36:28 PM.
This article is licensed under a Creative Commons Attribution-NonCommercial 3.0 Unported Licence.

Table 1 Antiproliferative activity on A2780, A2780cis, OVCAR-5, KURAMOCHI and MRC-5 cell lines

Compound	IC_{50} (μM)					Selectivity Index S.I.
	A2780	A2780*cis*	OVCAR-5	KURAMOCHI	MRC-5	
Cisplatin	0.26 ± 0.04	15 ± 1	1.04 ± 0.01	2.7 ± 0.5	2.4 ± 0.2	0.51
1	1.7 ± 0.3	1.6 ± 0.1	2.0 ± 0.2	3 ± 1	>100	>48
2	2.8 ± 0.5	4.00 ± 0.06	5.8 ± 0.4	3.3 ± 0.5	>100	>25
3	0.63 ± 0.03	2.4 ± 0.3	3.5 ± 0.1	2.6 ± 0.6	>100	>44
4	17 ± 2	3.3 ± 0.3	>100	>100	>100	>1.8
5	1.4 ± 0.5	0.55 ± 0.08	1.02 ± 0.07	7.3 ± 0.8	>100	>39
6	0.20 ± 0.05	0.31 ± 0.09	0.72 ± 0.07	0.3 ± 0.2	3.8 ± 0.2	9.9
7	0.27 ± 0.02	0.7 ± 0.1	3.42 ± 0.08	1.0 ± 0.2	3.1 ± 0.2	2.3
8	1.6 ± 0.9	2.7 ± 0.1	5.7 ± 0.8	3.0 ± 0.4	>100	>31
9	3.8 ± 0.6	3.5 ± 0.9	8.3 ± 0.5	8.4 ± 0.2	>100	>17
10	2.7 ± 0.3	3.8 ± 0.2	4.5 ± 0.1	4.3 ± 0.7	>100	>26
11	2.1 ± 0.2	2.8 ± 0.1	9 ± 2	7.7 ± 0.7	>100	>19
12	5.0 ± 0.6	43 ± 2	>100	>100	>100	>1.6
13	0.30 ± 0.04	1.02 ± 0.09	3.9 ± 0.1	0.72 ± 0.08	>100	>67
14	3.9 ± 0.3	4 ± 1	9 ± 1	5.1 ± 0.3	>100	>18
Juglone	3.6 ± 0.3	18 ± 2	5.1 ± 0.3	1.8 ± 0.2	30.0 ± 0.5	4.2

Data after 96 h of incubation. Stock solutions in DMSO for all complexes; stock solutions in H_2O for cisplatin. A2780 (cisplatin-sensitive ovarian cancer cells), A2780*cis* (cisplatin-resistant ovarian cancer cells), OVCAR-5 and KURAMOCHI (high-grade serous ovarian cancer cells), MRC-5 (normal lung fibroblasts). Cells were placed in 96 well plates and treated after 24 h with six different concentrations of Pd(II) complexes (0.001, 0.01, 0.1, 1, 10, 100) μM. After 96 h from the treatment cell viability was measured with a CellTiter glow assay (Promega, Madison, WI, USA; 1 : 1 dilution in PBS, 20 μL per well). Averages were obtained from triplicates and error bars are standard deviations. The selectivity index was calculated as the ratio between the IC_{50} determined in the non-tumor cell line and the mean IC_{50} obtained across the tumor cell lines investigated.

8, the cytotoxicity towards MRC-5 cells is one order of magnitude lower than that recorded for ovarian cancer cells. In fact, all complexes show a selectivity index (SI) exceeding that of cisplatin, with values ranging from 1.6 to >67. This finding seems to suggest a certain degree of selectivity of action towards malignant cells by our palladium(0) derivatives.

(c) In most cases, the synthesized complexes exhibit comparable cytotoxicity against both the cisplatin-sensitive A2780 and the cisplatin-resistant A2780*cis* cell lines. This observation suggests a mechanism of action for our palladium(0) compounds differs from that of cisplatin and, in any case, offers hope that they could also be effective against relapsed forms of ovarian cancer, for which treatment with platinum-based drugs is ineffective.

(d) Regarding the influence of the phosphine ancillary ligand on the biological activity of the corresponding Pd(0) complexes, no significant differences in IC_{50} values can be observed, regardless of the nature of the *para*-substituent in the case of the monodentate aryl phosphines (compounds **8–11**) or of the bite angle in the case of the bidentate ones (compounds **1–5**). Among the latter, however, it is worth noting the negative effect of DPPF, whose ferrocenyl structure appears to significantly lower the antiproliferative activity of complex **4**. Curiously, replacing one or both phosphorus donor atoms of dppe with arsenic atoms leads to a considerable increase in anticancer activity (**6** and **7** *vs.* **1**). This effect cannot be simply attributed to the presence of arsenic in the two compounds, as indirectly demonstrated by the fact that the complex coordinating two monodentate triphenylarsine ligands (**12**) is significantly less active than those bearing two triphenylphosphine ligands (**8**). Apparently, it is the combination of the nature of the donor atoms and the structure of the ancillary ligand that confers to complexes **6** and **7** their particularly high cytotoxicity. Unfortunately, this effect is at least partially observed also in the case of non-cancerous MRC-5 cells.

(e) The IC_{50} values recorded for free Juglone confirm its intrinsic anticancer activity. Specifically, the cytotoxicity of this olefin is comparable to that of most palladium(0) derivatives in the A2780, OVCAR-5, and KURAMOCHI cancer cell lines. Conversely, the antiproliferative activity of Juglone is markedly lower than that of its Pd(0) complexes when cisplatin-resistant A2780*cis* cells are considered. Moreover, it retains a certain degree of cytotoxicity towards non-cancerous MRC-5 cells (IC_{50} = 30 μM). It is important to emphasize that, among all the tested complexes, **6**, **7**, and **13** consistently exhibit IC_{50} values in ovarian cancer cells that are significantly lower than those of free Juglone, suggesting that, at least in these cases, the desired Juglone–palladium synergistic effect may indeed be operative.

Influence on PIN1 level in ovarian cancer cells

It is well known that the peptidyl-prolyl *cis–trans* isomerase NIMA-interacting 1 protein (PIN1) plays a fundamental role in regulating different cellular process, such as cell cycle progression, apoptosis, and signal transduction.[64] Moreover, it is ascertained that PIN1 is a critical regulator in the pathogenesis of ovarian cancer, modulating the localization, stability, and activity of several oncogenic proteins (cyclin D1, β-catenin, and NF-κB) and contextually inhibiting some important tumor suppressors (p53 and FOXO3a).[65] Therefore, overexpression of

Open Access Article. Published on 04 December 2025. Downloaded on 12/24/2025 9:36:28 PM.
This article is licensed under a Creative Commons Attribution-NonCommercial 3.0 Unported Licence.

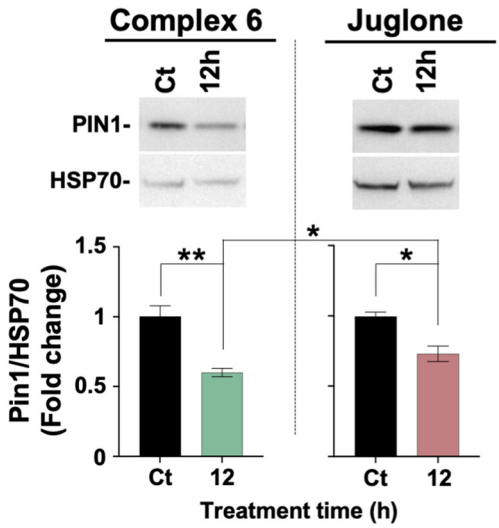

Fig. 4 Quantification of PIN1 protein levels by western blot in OVCAR-5 cells treated with 6 (1 μM) or Juglone (10 μM).

PIN1 has been correlated with enhanced cellular proliferation, resistance to apoptosis, and poor clinical prognosis.[66]

Juglone was the first identified PIN1 inhibitor. The inhibitory mechanism of Juglone involves irreversible covalent modification of a cysteine residue (Cys113) located within the conserved domain of PIN1. This is achieved through a Michael addition of cysteine thiol to olefinic group of Juglone.[52] Based on this knowledge it was decided to investigate if our Pd(0) complexes were also able to limit the activity of PIN1 inside ovarian cancer cells. For this study, it was selected complex **6** as model compound, since it showed the highest antitumor activity among the tested complexes, with IC_{50} values about one order of magnitude lower than those of free Juglone. The approach fielded to address the issue was based on western-blot analysis carried out on OVCAR-5 ovarian cancer cells. The experiment, in addition to complex **6**, covered also free Juglone.

Complex **6** (1 μM) and Juglone (10 μM) both induced a marked reduction in PIN1 protein levels in OVCAR-5 ovarian cancer cells, as shown by western blot analysis. Specifically, complex **6** markedly reduced PIN1 levels at 12 hours, comparable to or even slightly more effectively than Juglone, which showed a milder reduction at the same time point despite being used at a tenfold higher concentration (Fig. 4).[67]

These findings highlight the potential of complex **6** as a potent PIN1 inhibitor and support its further investigation alongside Juglone for therapeutic strategies targeting PIN1-dependent oncogenic pathways.

Conclusions

In this work, we have established the most suitable synthetic protocol for the preparation of a library of palladium(0)-η^2-Juglone complexes equipped with a wide range of ancillary ligands, including monodentate and bidentate phosphines or arsines, isocyanides, and functionalized N-heterocyclic carbenes. All compounds have been thoroughly characterized using spectroscopic techniques and, in selected cases, by X-ray diffraction. The aim of this synthetic effort was the preparation of derivatives simultaneously incorporating two different anticancer components, namely Juglone—an organic molecule that acts as a PIN1 inhibitor—and the palladium(0) fragment, which we have previously proven to be an effective antiproliferative agent against many types of ovarian tumour cells.

In vitro tests conducted on different ovarian cancer cell lines revealed that most of the prepared compounds are capable of promoting an efficient antiproliferative activity, with IC_{50} values similar to those of cisplatin. However, our palladium(0) complexes display markedly lower cytotoxicity towards MRC-5 non-cancerous cells compared to cisplatin, suggesting a certain degree of selectivity towards ovarian cancer cells. Another encouraging result is the very similar activity of our complexes towards both A2780 and A2780*cis* cells, suggesting the possibility of employing them even in relapsed forms of ovarian cancer unresponsive to a second treatment with platinum-based drugs.

Finally, comparison between the cytotoxicity of free Juglone and that of our palladium(0) derivatives allowed us to identify at least three metal compounds (**6**, **7**, and **13**) whose IC_{50} values are significantly lower across all ovarian cancer cell lines tested. This result provides evidence of the synergistic effect we were hoping for. Certainly, it is not an easy task to provide a clear rationale for this combined effect, but western blot experiments conducted on complex **6** have shown that the Juglone inhibitory effect on the PIN1 key protein persists even after its coordination to the palladium(0) metal centre. This may be due to the fact that coordination of Juglone could facilitate the attack of the cysteine residue (Cys113) thiol of PIN1, resulting in protein deactivation. Moreover, it is likely that after this nucleophilic attack, a palladium(0) residue might be released inside the cell, promoting an independent cytotoxic effect.

Based on these findings, we are planning to carry out further studies in our laboratories to verify whether the most promising palladium(0)-η^2-Juglone complexes retain their anticancer properties even in more complex biological systems, such as patient-derived organoids and animal models. Should the results prove positive, we will attempt to gain deeper insights into their precise mode of action.

Experimental

Solvents and reagents

All syntheses were carried out under Argon atmosphere using standard Schlenk techniques. Dichloromethane and acetone were treated with 4 Å molecular sieves. All other solvents and chemicals were commercial grade products and used as purchased. The precursors $[Pd_2(dba)_3{\cdot}CHCl_3]$ (dba = dibenzylideneacetone) and [(*N*-1-mesityl-(2-pyridylmethyl)imidazol-

Open Access Article. Published on 04 December 2025. Downloaded on 12/24/2025 9:36:28 PM.
This article is licensed under a Creative Commons Attribution-NonCommercial 3.0 Unported Licence.

2ylidene)AgBr][68] were synthesized according to published protocols.

NMR, IR and elemental analyses

1D-NMR and 2D-NMR spectra were recorded on Bruker 300 or 400 Advance spectrometers. Chemical shifts values (ppm) are given relative to TMS (^{1}H and ^{13}C), H_3PO_4 (^{31}P) and CCl_3F (^{19}F).

IR spectra were recorded on a PerkinElmer Spectrum One spectrophotometer. Elemental analyses were carried out using an Elemental CHN "CUBO Micro Vario" analyzer.

Crystal structure determination

5, **7** and **13** crystals data were collected at XRD2 beamline of the Elettra Synchrotron, Trieste (Italy),[69] using a monochromatic wavelength of 0.620 Å, at 100 K or 298 K. The data sets were integrated, scaled and corrected for Lorentz, absorption and polarization effects using XDS package.[70] Data from two random orientations of the same crystals have been merged to obtain complete datasets for the triclinic **5** crystal form, using CCP4-Aimless code.[71,72] The structures were solved by direct methods using SHELXT program[73] and refined using full-matrix least-squares implemented in SHELXL-2019/3.[74] Thermal motions for all non-hydrogen atoms have been treated anisotropically when occupancies were higher than 45%. Hydrogens have been included on calculated positions, riding on their carrier atoms. Geometric restrains (SAME, SADI, DFIX, DANG) have been applied to disordered fragments (phosphine ligand in **7** and solvent in **5** and **7**). The Coot program was used for structure building.[75] The crystal data are given in Table S1 in SI. Pictures were prepared using Ortep3[76] and Pymol[77] software. Crystallographic data have been deposited at the Cambridge Crystallographic Data Centre and allocated the deposition number CCDC 2441626 (**5** at 100 K), 2441623 (**7** at 100 K), 2441624 (**13** at 100 K) and 2441625 (**13** at 298 K).

Synthesis of palladium(η^2-Juglone) complexes

[Pd(η^2-Juglone)(NSPM)] (A). Anhydrous acetone (45 mL) was introduced in a 100 mL round-bottom-flask under inert argon atmosphere, and, in sequence, NSPM (Me-py-CH_2-SPh) (138.6 mg, 0.6444 mmol), Juglone (112.9 mg, 0.6483 mmol) and [$Pd_2(dba)_3$·$CHCl_3$] (303.3 mg, 0.2930 mmol) were added. After one hour, during which time the colour of the reaction mixture changed from purple to orange/red, the resulting solution was treated with activated carbon and filtered on millipore. After removing the solvent under vacuum, the solid was treated with anhydrous diethyl ether, separated by filtration and washed with anhydrous diethyl ether and *n*-pentane. Finally, the dark orange solid was dried in vacuum. 249.7 mg of product was obtained, corresponding to a 83% yield.

^{1}H NMR (300 MHz, $CDCl_3$, *T* = 298 K, ppm) δ: 2.79 (s, 3H, CH_3), 4.36 (s, 2H, SCH_2), 4.89 (s, 2H, CH═CH), 6.98–7.59 (m, 11H, Ar–H), 13.10 (s, 1H, OH).

^{13}C{^{1}H} NMR (75 MHz, $CDCl_3$, *T* = 298 K, ppm) δ: 27.1–28.1 (CH_3, py–CH_3), 45.5 (CH_2, SCH_2), 58.2 (CH, CH═CH, not detectable), 64.3 (CH, CH═CH, not detectable), 117.3–118.0 (CH, C^4), 120.3–120.6 (C, C^{7a}), 122.1–123.8 (CH, py–C^5, py–C^3), 128.0–129.1 (CH, CH–Ph), 129.3 (CH, CH–Ph), 130.9–131.2 (CH, C^5), 134.0–135.1 (C, C^{3a}), 137.7–138.1 (CH, py–C^4), 156.8 (C, py–C^6), 161.1–161.7 (C, C^7, py–C^2), 184.9–185.3 (C, C^3), 190.7 (C, C^8).

IR (KBr pellet, cm^{-1}): 1609 ν(CO).

[Pd(η^2-Juglone)(dppe)] (1). In a round-bottom flask equipped with a magnetic stirrer, [Pd(η^2-Juglone)(NSPM)] (70.3 mg, 0.142 mmol) was dissolved in anhydrous dichloromethane (7 mL) under inert argon atmosphere, giving a violet/red solution. Then, a dichloromethane solution of 1,2-bis(diphenylphosphine)ethane (59.2 mg, 0.149 mmol, 1.04 eq., 5 mL) was added to the reaction flask under magnetic stirring. The rapid colour change of the solution towards red was observed. The system was kept under magnetic agitation at room temperature for about fifteen minutes, after which the reaction mixture was filtered on millipore and the solvent was removed in vacuum. The red solid residue was treated with anhydrous diethyl ether, filtered and washed with several aliquots of anhydrous diethyl ether and *n*-pentane. The product was finally dried in vacuum at room temperature.

86.9 mg of [Pd(dppe)(η^2-Juglone)] were obtained, corresponding to a 90% yield.

^{1}H NMR (300 MHz, $CDCl_3$, *T* = 298 K, ppm) δ: 1.99–2.46 (m, 4H, PCH_2), 5.14–5.24 (m 2H, CH═CH), 6.99–7.75 (m, 23H Ar–H), 13.40 (s, 1H, OH).

^{13}C{^{1}H} NMR (75 MHz, $CDCl_3$, *T* = 298 K, ppm) δ: 26.1–26.7 (CH_2, m, PCH_2), 69.9 (CH, dd, J_{C-P} = 10.8, 6.8 Hz, CH═CH), 70.5 (CH, dd, J_{C-P} = 9.1, 4.9, CH═CH), 116.7 (CH, C^4) 119.3 (C, C^{7a}), 120.5 (CH, C^6), 128.8–128.9 (m), 129.1–129.4 (m), 130.7, 130.9, 131.0, 132.3–132.7 (m), 133.3, 137.1 (CH, C^{3a}), 161.0 (C, C^7), 182.7 (C, C^3), 187.8 (C, C^8).

^{31}P{^{1}H} NMR (121 MHz, $CDCl_3$, *T* = 298 K, ppm) δ: 41.4.

IR (KBr pellet, cm^{-1}): 1594 ν(CO).

Elemental analysis calcd (%) for $C_{36}H_{30}O_3P_2Pd$: C, 63.68, H, 4.45; found: C, 63.84, H, 4.31.

[Pd(η^2-Juglone)(dppp)] (2). Complex **2** was obtained in the same way of complex **1** employing a dichloromethane solution of [Pd (η^2-Juglone)(NSPM)] (70.0 mg, 0.141 mmol, 7 mL) and a dichloromethane solution of 1,2-bis(diphenylphosphine) propane (60.6 mg, 0.147 mmol, 5 mL). 89.3 mg of product was obtained as dark orange solid, corresponding to a yield of 91%.

^{1}H NMR (300 MHz, $CDCl_3$, *T* = 298 K, ppm) δ: 1.53–1.63 (m, 2H, CH_2), 2.22–2.31 (m, 2H, PCH_2), 2.45–2.62 (m, 2H, PCH_2), 4.68–4.78 (m, 2H, CH═CH), 6.98–7.62 (m, 23H, Ar–H), 13.22 (s, 1H, OH).

^{13}C{^{1}H} NMR (75.0 MHz, $CDCl_3$, *T* = 298 K, ppm) δ: 19.3–19.4 (CH_2, m, CH_2), 28.1–28.6 (CH_2, m, PCH_2), 69.5 (CH, d, J_{C-P} = 15.8 Hz, CH═CH), 70.1 (CH, d, J_{C-P} = 13.5 Hz, CH═CH), 116.9 (CH, C^4) 119.1 (C, C^{7a}), 120.5 (CH, C^6), 128.4, 128.5, 128.7, 128.8, 130.2, 130.4, 130.6, 132.0, 132.1, 133.1, 133.2, 133.3, 133.4, 137.0 (CH, C^{3a}), 161.0 (C, C^7), 183.1 (C, d, J_{C-P} = 5.7 Hz, C^3), 188.4 (C, J_{C-P} = 4.1 Hz, C^8).

^{31}P{^{1}H} NMR (121 MHz, $CDCl_3$, *T* = 298 K, ppm) δ: 11.5 (d, J_{P-P} = 65.7 Hz), 12.1 (d, J_{P-P} = 65.7 Hz).

Open Access Article. Published on 04 December 2025. Downloaded on 12/24/2025 9:36:28 PM.
This article is licensed under a Creative Commons Attribution-NonCommercial 3.0 Unported Licence.

IR (KBr pellet, cm^{-1}): 1602 ν(CO).

Elemental analysis calcd (%) for $C_{37}H_{32}O_3P_2Pd$: C, 64.13, H, 4.65; found: C, 63.72, H, 4.80.

[Pd(η^2-Juglone)(dppbz)] (3). Complex **3** was obtained in the same way of complex **1** employing a dichloromethane solution of [Pd (η^2-Juglone)(NSPM)] (70.2 mg, 0.142 mmol, 7 mL) and a dichloromethane solution of 1,2-bis(diphenylphosphine) benzene (65.6 mg, 0.147 mmol, 5 mL). 77.1 mg of product was obtained as dark orange solid, corresponding to a yield of 75%.

^{1}H NMR (300 MHz, CDCl$_3$, *T* = 298 K, ppm) δ: 5.03–5.12 (m, 2H, CH═CH), 6.89–7.64 (m, 27H, Ar–H), 13.33 (s, 1H, OH).

^{13}C{^{1}H} NMR (75.0 MHz, CDCl$_3$, *T* = 298 K, ppm) δ: 71.1 (CH, d, J_{C-P} = 11.6, 5.5 Hz, CH═CH), 71.4 (CH, d, J_{C-P} = 10.1, 3.8 Hz, CH═CH), 116.5 (CH, C^4), 119.2 (C, C^{7a}), 120.3 (CH, C^6), 128.6–128.8 (m), 129.0–129.2 (m), 130.3, 130.5, 130.6, 131.5, 132.5–133.1 (m), 134.2–134.4 (m), 136.9 (C, C^{3a}), 160.8 (C, C^7), 181.6 (C, C^3), 187.0 (C, C^8).

^{31}P{^{1}H} NMR (121 MHz, CDCl$_3$, *T* = 298 K, ppm) δ: 44.5 (d, J_{P-P} = 37.1 Hz), 44.6 (d, J_{P-P} = 37.1 Hz).

IR (KBr pellets, cm^{-1}): 1604 ν(CO).

Elemental analysis calcd (%) for $C_{40}H_{30}O_3P_2Pd$: C, 66.08, H, 4.16; found: C, 66.40, H, 4.04.

[Pd(η^2-Juglone)(dppf)] (4). Complex **4** was obtained in the same way of complex **1** employing a dichloromethane solution of [Pd (η^2-Juglone)(NSPM)] (70.7 mg, 0.143 mmol, 7 mL) and a dichloromethane solution of 1,1′-bis(diphenylphosphine)ferrocene (81.4 mg, 0.147 mmol, 5 mL). 90.7 mg of product was obtained as dark orange solid, corresponding to a yield of 76%.

^{1}H NMR (300 MHz, CDCl$_3$, *T* = 298 K, ppm) δ: 3.99–4.03 (m, 2H, Fc–CH), 4.10–4.12 (m, 1H, Fc–CH), 4.17–4.23 (m, 5H, Fc–CH), 4.62–4.71 (m, 2H, CH═CH), 6.86–7.79 (m, 23H, Ar–H), 12.38 (s, 1H, OH).

^{13}C{^{1}H} NMR (75 MHz, CDCl$_3$, *T* = 298 K, ppm) δ: 68.6 (CH, dd, J_{C-P} = 18.1, 1.1 Hz, CH═CH), 69.3 (CH, d, J_{C-P} = 16.5, 1.9 Hz, CH═CH), 72.2, 72.3, 72.3 72.4, 72.5, 72,6, 72.6, 72.7 (Fc–CH), 74.2, 74.3, 74.4, 74.5 (Fc–CH), 75.0, 75.1, 75.3 (Fc–CH), 116.9 (CH, C^4) 118.4 (C, C^{7a}), 120.5 (CH, C^6), 128.1, 128.2, 128.4, 128.5, 128.6, 128.6, 128.7, 129.7, 129.7, 130.1, 130.1, 130.4, 130.5, 130.6, 130.7, 132.3, 132.4, 132.5, 132.6, 133.0, 133.0, 133.2, 133.3, 133.4, 133.6, 134.0, 134.2, 134.5, 134.7, 134.9, 135.0, 135.4, 135.5, 135.6, 135.7, 136.0, 136.1, 136.5, 136.6, 160.3 (C, C^7), 183.1 (C, dd, J_{C-P} = 5.1, 1.4 Hz, C^3), 188.8 (C, dd, J_{C-P} = 5.2, 1.5 Hz, C^8).

^{31}P{^{1}H} NMR (121 MHz, CDCl$_3$, *T* = 298 K, ppm) δ: 24.3 (d, J_{P-P} = 42.9 Hz), 25.1 (d, J_{P-P} = 42.9 Hz).

IR (KBr pellet, cm^{-1}): 1607 ν(CO).

Elemental analysis calcd (%) for $C_{44}H_{34}FeO_3P_2Pd$: C, 63.29, H, 4.10; found: C, 63.51, H, 3.99.

[Pd(η^2-Juglone)(DPEphos)] (5). Complex **5** was obtained in the same way of complex **1** employing a dichloromethane solution of [Pd (η^2-Juglone)(NSPM)] (71.2 mg, 0.144 mmol, 7 mL) and a dichloromethane solution of bis[(diphenylphosphine) phenyl]ether (79.3 mg, 0.147 mmol, 5 mL). 105.0 g of product was obtained as dark orange solid, corresponding to a yield of 89%.

^{1}H NMR (300 MHz, CDCl$_3$, *T* = 298 K, ppm) δ: 4.69–4.78 (m, 2H, CH═CH), 6.41–7.46 (m, 31H, Ar–H), 12.23 (s, 1H, OH).

^{13}C{^{1}H} NMR (75.0 MHz, CDCl$_3$, *T* = 298 K, ppm) δ: 68.9–69.6 (m, CH, CH═CH), 117.1 (CH, C^4), 118.6, 120.0, 120.5, 121.1, 124.4, 124.8, 128.1, 128.2, 128.4, 128.5, 128.6, 128.8, 129.9, 131.4, 133.2, 133.4, 133.5, 133.6, 133.7, 133.8, 134.6, 135.1, 136.5, 158.9, 159.0, 159.1, 159.2, 160.3 (C, C^7), 183.4 (C, C^3), 188.9. (C, C^8).

^{31}P{^{1}H} NMR (121 MHz, CDCl$_3$, *T* = 298 K, ppm) δ: 16.8 (d, J_{P-P} = 31.2 Hz), 18.4 (d, J_{P-P} = 31.2 Hz).

IR (KBr pellets, cm^{-1}): 1611 ν(CO).

Elemental analysis calcd (%) for $C_{46}H_{34}O_4P_2Pd$: C, 67.45, H, 4.18; found: C, 67.12, H, 4.30.

[Pd(η^2-Juglone)][Pd(Ph$_2$AsC$_2$H$_4$AsPh$_2$)] (6). Complex **6** was obtained in the same way of complex **6** employing a dichloromethane solution of [Pd (η^2-Juglone)(NSPM)] (70.3 mg, 0.141 mmol, 7 mL) and a dichloromethane solution of bis[(2-diphenilarsine)phenyl]ethane (59.2 mg, 0.149 mmol, 5 mL). 95.9 mg of product was obtained as dark orange solid, corresponding to a yield of 88%.

^{1}H NMR (300 MHz, CDCl$_3$, *T* = 298 K, ppm) δ: 2.18 (s, 4H, AsCH$_2$) 5.40–5.43 (AB system, *J* = 7.4 Hz, 2H, CH═CH), 7.01–7.58 (m, 23H, Ar–H), 13.24 (s, 1H, OH).

^{13}C{^{1}H} NMR (75.0 MHz, CDCl$_3$, *T* = 298 K, ppm) δ: 23.7 (CH$_2$, AsCH$_2$), 68.4 (CH, CH═CH), 68.9 (CH, CH═CH), 116.9 (CH, C^4), 118.9 (C, C^{7a}), 121.1 (CH, C^6), 129.4, 130.4, 132.4, 133.8, 134.9, 136.6 (CH, C^{3a}), 160.9 (C, C^7), 184.1 (C, C^3), 189.5 (C, C^8).

IR (KBr pellet, cm^{-1}): 1604 ν(CO).

Elemental analysis calcd (%) for $C_{36}H_{30}As_2O_3Pd$: C, 56.38, H, 3.94; found: C, 56.54, H, 3.79.

[Pd(η^2-Juglone)][Pd(Ph$_2$AsC$_2$H$_4$PPh$_2$)] (7). Complex **7** was obtained in the same way of complex **1** employing a dichloromethane solution of [Pd (η^2-Juglone)(NSPM)] (70.3 mg, 0.142 mmol, 7 mL) and a dichloromethane solution of bis[(1-diphenylphosphine,2-diphenilarsine)phenyl]ethane (59.2 mg, 0.149 mmol, 5 mL). 86.9 mg of product was obtained as dark orange solid, corresponding to a yield of 90%.

^{1}H NMR (300 MHz, CDCl$_3$, *T* = 298 K, ppm) δ: 1.89–2.40 (m, 8H, CH$_2$), 5.25–5.36 (m, 4H, CH═CH), 7.01–7.73 (m, 46H, Ar–H), 13.21 (s, 1H, OH), 13.41 (s, 1H, OH).

^{13}C{^{1}H} NMR (75.0 MHz, CDCl$_3$, *T* = 298 K, ppm) δ: 23.6 (CH, d, J_{C-P} = 10.8 Hz, AsCH$_2$), 23.8 (CH, d, J_{C-P} = 11.3 Hz, AsCH$_2$), 26.0 (CH, d, J_{C-P} = 15.4 Hz, PCH$_2$), 26.4 (CH, d, J_{C-P} = 15.6 Hz, PCH$_2$), 68.3 (CH, d, J_{C-P} = 18.7 Hz, CH═CH), 68.9 (CH, d, J_{C-P} = 16.6 Hz, CH═CH), 69.7 (CH, d, J_{C-P} = 1.3 Hz, CH═CH), 70.3 (CH, d, J_{C-P} = 2.3 Hz, CH═CH), 116.6 (CH, C^4), 116.7 (CH, C^4), 118.9 (C, d, J_{C-P} = 1.5 Hz, C^{7a}), 119.0 (C, C$_{7a}$), 120.6 (CH, C^6), 120.7 (CH, C^6), 128.6, 128.8, 128.9, 129.0, 129.0, 129.0, 129.1, 129.2, 129.2, 129.3, 129.4, 130.1, 130.3, 130.4 130.4, 130.5, 130.6, 130.7, 130.7, 130.8, 131.7, 132.1, 132.2, 132.2, 132.3, 132.3, 132.3, 132.4, 132.4, 132.5, 132.5, 132.6, 133.0, 133.1, 133.4, 134.3, 134.3, 134.5, 134.6, 134.6, 136.7 (C, d, J_{C-P} = 1.2 Hz, C^{3a}), 136.7 (C, C^{3a}), 160.8 (C, C^7),

Open Access Article. Published on 04 December 2025. Downloaded on 12/24/2025 9:36:28 PM.
This article is licensed under a Creative Commons Attribution-NonCommercial 3.0 Unported Licence.

160.9 (C, C^7), 182.8 (C, C^3), 183.9 (C, d, J_{C-P} = 7.1 Hz, C^3), 188.1 (C, C^8), 189.2 (C, d, J_{C-P} = 5.8 Hz, C^8).

$^{31}P\{^1H\}$ NMR (121 MHz, $CDCl_3$, T = 298 K, ppm) δ: 43.0, 43.1.

IR (KBr pellets, cm^{-1}): 1600 ν(CO).

Elemental analysis calcd (%) for $C_{36}H_{30}AsO_3PPd$: C, 59.81, H, 4.18; found: C, 59.60, H, 4.29.

[Pd(η^2-Juglone)(PPh_3)$_2$] (8). In a round-bottom flask 70.6 mg (0.142 mmol) of [Pd (η^2-Juglone)(NSPM)] were dissolved in 7 mL of dichloromethane anhydrous under argon atmosphere, obtaining a violet/red solution, to which 78.5 mg (0.299 mmol, 2.08 eq.) of triphenylphosphine, dissolved in 5 mL of dichloromethane anhydrous, were added. The sudden colour change of the solution towards dark red was observed. The system was kept under magnetic stirring at room temperature for 15 minutes, after which it was filtered on millipore and subsequently the solvent was removed under vacuum. The residue was treated with anhydrous diethyl ether, filtered and washed with little aliquots first of anhydrous diethyl ether and then of *n*-pentane. Finally, the solid was dried in vacuum at room temperature. 90.3 mg of [Pd(η^2-Juglone)(PPh_3)$_2$] was obtained, corresponding to a yield of 79%.

^1H NMR (300 MHz, $CDCl_3$, T = 298 K, ppm) δ: 4.60–4.67 (m, 2H, CH═CH), 6.96–7.37 (m, 33H, Ar–H), 12.46 (s, 1H, OH).

$^{13}C\{^1H\}$ NMR (75.0 MHz, $CDCl_3$, T = 298 K, ppm) δ: 69.3 (CH, d, J_{C-P} = 18.2 Hz, CH═CH), 69.9 (CH, d, J_{C-P} = 15.5 Hz, CH═CH), 117.0 (CH, C^4) 118.3 (C, C^{7a}), 120.8 (CH, C^6), 128.1, 128.2, 128.4, 129.7, 132.2, 132.3, 132.7, 133.1, 133.5, 133.6, 133.7, 133.8, 133.8, 136.4 (CH, C^{3a}), 160.6 (C, C^7), 183.7 (C, d, J_{C-P} = 5.0 Hz, C^3), 189.5 (C, d, J_{C-P} = 4.5 Hz, C^8).

$^{31}P\{^1H\}$ NMR (121 MHz, $CDCl_3$, T = 298 K, ppm) δ: 28.9 (d, J_{P-P} = 25.6 Hz), 29.6 (d, J_{P-P} = 25.6 Hz).

IR (KBr pellets, cm^{-1}): 1612 ν(CO).

Elemental analysis calcd (%) for $C_{46}H_{36}O_3P_2Pd$: C, 68.62, H, 4.51; found: C, 68.89, H, 4.34.

[Pd((η^2-Juglone)(P(*p*-Cl-C_6H_4)$_3$)$_2$)] (9). Complex **9** was obtained in the same way of complex **8** employing a dichloromethane solution of [Pd (η^2-Juglone)(NSPM)] (70.2 mg, 0.142 mmol, 7 mL), and a dichloromethane solution of tris-(4-chlorophenyl)phosphine (108.4 mg, 0.296 mmol, 5 mL). 91.1 mg of product was obtained as dark orange solid, corresponding to a yield of 64%.

^1H NMR (300 MHz, $CDCl_3$, T = 298 K, ppm) δ: 4.66–4.74 (m, 2H, CH═CH), 6.94–7.19 (m, 33H, Ar–H), 12.31 (s, 1H, OH).

$^{13}C\{^1H\}$ NMR (75.0 MHz, $CDCl_3$, T = 298 K, ppm) δ: 70.0 (CH, d, J_{C-P} = 18.0 Hz, CH═CH), 70.3 (CH, d, J_{C-P} = 14.9 Hz, CH═CH), 117.0 (CH, C^4) 117.6 (C, C^{7a}), 121.4 (CH, C^6), 128.7, 128.8, 128.9, 129.1, 129.2, 130.2, 130.7, 133.3, 133.4, 134.2, 134.3, 134.4, 134.5, 135.6 (CH, C^{3a}), 136.9, 160.7 (C, C^7), 183.7 (C, d, J_{C-P} = 5.1 Hz, C^3), 189.9 (C, d, J_{C-P} = 4.4 Hz, C^8).

$^{31}P\{^1H\}$ NMR (121 MHz, $CDCl_3$, T = 298 K, ppm) δ: 26.8 (d, J_{P-P} = 16.1 Hz), 27.4 (d, J_{P-P} = 16.1 Hz).

IR (KBr pellets, cm^{-1}): 1612 ν(CO).

Elemental analysis calcd (%) for $C_{46}H_{30}Cl_6O_3P_2Pd$: C, 54.61, H, 2.99; found: C, 54.27, H, 3.11.

[Pd(η^2-Juglone)((P(*p*-OMe-C_6H_4)$_3$)$_2$)] (10). Complex **10** was obtained in the same way of complex **8** employing a dichloromethane solution of [Pd (η^2-Juglone)(NSPM)] (70.2 mg, 0.142 mmol, 7 mL) and a dichloromethane solution of tris-(4-methoxyphenyl) phosphine (104.5 mg, 0.296 mmol, 5 mL). 85.1 mg of product was obtained as dark orange solid, corresponding to a yield of 61%.

^1H NMR (300 MHz, $CDCl_3$, T = 298 K, ppm) δ: 3.76 (s, 9H, OCH_3), 3.77 (s, 9H, OCH_3), 4.58–4.65 (m, 2H, CH═CH), 6.63–7.37 (m, 27H, Ar–H), 12.65 (s, 1H, OH).

$^{13}C\{^1H\}$ NMR (75 MHz, $CDCl_3$, T = 298 K, ppm) δ: 55.2 (CH_3, OCH_3), 55.3 (CH_3, OCH_3), 68.5 (CH, d, J_{C-P} = 17.5 Hz, CH═CH), 69.2 (CH, d, J_{C-P} = 15.5 Hz, CH═CH), 113.6, 113.8, 113.9, 116.9 (CH, C^4) 118.5 (C, C^{7a}), 120.5 (CH, C^6), 124.4–124.6 (m), 124.9–125.1 (m), 133.2, 133.9, 134.1, 134.9, 135.0, 135.1, 135.2, 136.6 (CH, C^{3a}), 160.6 (C, C^7), 183.5 (C, d, J_{C-P} = 5.0 Hz, C^3), 189.4 (C, d, J_{C-P} = 3.3 Hz, C^8).

$^{31}P\{^1H\}$ NMR (121 MHz, $CDCl_3$, T = 298 K, ppm) δ: 25.9 (d, J_{P-P} = 32.0 Hz), 26.4 (d, J_{P-P} = 32.0 Hz).

IR (KBr pellet, cm^{-1}): 1590 ν(CO).

Elemental analysis calcd (%) for $C_{52}H_{48}O_9P_2Pd$: C, 63.39, H, 4.91; found: C, 63.60, H, 4.78.

[Pd(η^2-Juglone)((P(*p*-F-C_6H_4)$_3$)$_2$)] (11). Complex **11** was obtained in the same way of complex **8** employing a dichloromethane solution of [Pd (η^2-Juglone)(NSPM)] (71.9 mg, 0.145 mmol, 7 mL) and a dichloromethane solution of tris-(4-fluorophenyl)phoshine (93.8 mg, 0.296 mmol, 5 mL). 65.5 mg of product was obtained as dark orange solid, corresponding to a yield of 51%.

^1H NMR (300 MHz, $CDCl_3$, T = 298 K, ppm) δ: 4.63–4.71 (m, 2H, CH═CH), 6.85–7.69 (m, 27H, Ar–H), 12.36 (s, 1H, OH).

$^{13}C\{^1H\}$ NMR (75 MHz, $CDCl_3$, T = 298 K, ppm) δ: 69.6 (CH, d, J_{C-P} = 17.8 Hz, CH═CH), 70.1 (CH, d, J_{C-P} = 16.5 Hz, CH═CH), 115.6–116.5 (m), 117.1, 118.0 (C, C^{7a}), 121.4 (CH, C^6), 128.1, 128.6, 133.9, 134.5, 134.6, 134.8, 135.3–135.7 (m), 136.0 (C, C^{3a}), 160.8 (C, C^7), 162.3, 165.6, 183.8 (C, d, J_{C-P} = 4.6 Hz, C^3), 189.9 (C, d, J_{C-P} = 3.0 Hz, C^8).

$^{31}P\{^1H\}$ NMR (121 MHz, $CDCl_3$, T = 298 K, ppm) δ: 26.4 (dq, J_{P-P} = 19.8, J_{P-F} = 3.2 Hz), 27.0 (d, J_{P-P} = 19.8 Hz, J_{P-F} = 3.2 Hz).

$^{19}F\{^1H\}$ NMR (377 MHz, $CDCl_3$, T = 298 K, ppm) δ: −109.2 (d, J_{F-P} = 3.2 Hz), −109.1 (d, J_{F-P} = 3.4 Hz).

IR (KBr pellet, cm^{-1}): 1590 ν(CO).

Elemental analysis calcd (%) for $C_{46}H_{30}F_6O_3P_2Pd$: C, 60.51, H, 3.31; found: C, 60.19, H, 3.43.

[Pd(η^2-Juglone)($AsPh_3$)$_2$] (12). Complex **12** was obtained in the same way of complex **8** employing a dichloromethane solution of [Pd (η^2-Juglone)(NSPM)] (70.9 mg, 0.141 mmol, 7 mL) and a dichloromethane solution of triphenylarsine (90.0 mg, 0.294 mmol, 5 mL). 66.4 mg of product was obtained as dark orange solid, corresponding to a yield of 60%.

^1H NMR (300 MHz, $CDCl_3$, T = 298 K, ppm) δ: 5.12–5.15 (AB system J = 7.6 Hz, 2H, CH═CH), 7.10–7.49 (m, 33H, Ar–H), 12.50 (s, 1H, OH).

$^{13}C\{^1H\}$ NMR (75 MHz, $CDCl_3$, T = 298 K, ppm) δ: 67.4 (CH, CH═CH), 68.1 (CH, CH═CH), 117.1 (CH, C^4) 118.1 (C, C^{7a}), 121.2 (CH, C^6), 128.7, 129.5, 131.6, 133.4, 133.8, 135.3, 136.1 (CH, C^{3a}), 160.5 (C, C^7), 184.1 (C, C^3), 189.8 (C, C^8).

Open Access Article. Published on 04 December 2025. Downloaded on 12/24/2025 9:36:28 PM.
This article is licensed under a Creative Commons Attribution-NonCommercial 3.0 Unported Licence.

IR (KBr pellets, cm^{-1}): 1611 ν(CO).

Elemental analysis calcd (%) for $C_{46}H_{36}As_2O_3Pd$: C, 61.87, H, 4.06; found: C, 62.06, H, 3.98.

[Pd(η^2-Juglone)(TIC)(PPh$_3$)] (13). In a round-bottom flask, [Pd (η^2-Juglone)(NSPM)] (78.1 mg, 0.157 mmol) was dissolved in 5 mL of anhydrous dichloromethane under argon atmosphere, resulting as a violet red solution. After that, a dichloromethane solution of *tert*-butyl-isocyanide (136.0 mg, 0.163 mmol, 1.04 eq., 2 mL) and a dichloromethane solution of triphenylphosphine (43.3 mg, 0.165 mmol, 1.04 eq., 5 mL) were added, observing a rapid colour change of the solution to dark orange. The reaction mixture was kept under magnetic agitation at room temperature for 45 minutes, after which it was filtered and the solvent was removed in vacuum. The resulting residue was treated with 4 mL of anhydrous diethyl ether and 8 mL of *n*-pentane, filtered and washed with anhydrous diethyl ether and *n*-pentane. The obtained orange solid was finally dried under vacuum.

87.0 mg of [Pd(η^2-Juglone)(TIC)(PPh$_3$)] was obtained, corresponding to a yield of 88%.

^{1}H NMR (300 MHz, CDCl$_3$, *T* = 298 K, ppm) δ: 1.25 (s, 18H, *t*-Bu-CH$_3$), 4.68–4.70 (m, 2H, CH═CH), 4.86–5.05 (m, 2H, CH═CH), 6.91–7.61 (m, 36H, Ar–H), 12.55 (s, 1H, OH) 13.43 (s, 1H, OH).

^{13}C{^{1}H} NMR (75.0 MHz, CDCl$_3$, *T* = 298 K, ppm) δ: 30.2 (CH$_3$, *t*-Bu–CH$_3$), 57.0 (C, *t*-Bu–C), 65.8 (CH, d, J_{C-P} = 1.5 Hz, CH═CH), 66.2 (CH, d, J_{C-P} = 2.6 Hz, CH═CH), 66.8 (CH, d, J_{C-P} = 18.2 Hz, CH═CH), 68.0 (CH, d, J_{C-P} = 15.9 Hz, CH═CH), 116.4 (CH, C^4), 117.1 (CH, C^4), 118.4 (C, C^{7a}), 118.7 (C, C^{7a}), 120.8 (CH, C^6), 121.0 (CH, C^6), 128.5–128.7 (m), 130.1, 133.2, 133.3, 133.5–133.8 (m), 136.3 (CH, C^{3a}), 136.6 (CH, C^{3a}), 160.6 (C, C^7), 160.9 (C, C^7), 184.4 (C, C^3), 184.7 (C, d, J_{C-P} = 6.4 Hz, C^3), 189.6 (C, d, J_{C-P} = 5.8 Hz, C^8), 190.3 (C, C^8).

^{31}P{^{1}H} NMR (121 MHz, CDCl$_3$, *T* = 298 K, ppm) δ: 28.8, 29.3.

IR (KBr pellet, cm^{-1}): 2172 ν(CN), 1607 ν(CO).

Elemental analysis calcd (%) for $C_{33}H_{30}NO_3PPd$: C, 63.32, H, 4.83, N, 2.24; found: C, 63.59, H, 4.72, N, 2.33.

[Pd(η^2-Juglone)(Mes-Im-CH$_2$Py)] (14). In a round-bottom flask, [Pd (η^2-Juglone)(NSPM)] (73.6 mg, 0.148 mmol) was dissolved in 14 mL of anhydrous dichloromethane under an argon atmosphere, obtaining a pink-violet solution. After that, a dichloromethane solution of [(Mes-Im-CH$_2$Py)AgBr] (69.0 mg, 0.0742 mmol, 1 eq., 10 mL) was slowly added drop by drop, maintaining the system under vigorous magnetic stirring. A progressive cloudiness of solution due to the precipitation of silver bromide was observed, accompanied by the simultaneous colour change of reaction mixture towards orange. The system was kept under magnetic stirring for 15 more minutes, after which the mixture was filtered, and the solvent was removed in vacuum. The solid residue was treated with 10 mL of anhydrous diethyl ether and, after filtration, firstly washed with anhydrous diethyl ether and then with *n*-pentane. Finally, the dark orange solid was dried in vacuum.

62.0 mg of [Pd(η^2-Juglone)(Mes-Im-CH$_2$Py)] was obtained, corresponding to a yield of 76%.

^{1}H NMR (300 MHz, CDCl$_3$, *T* = 253 K, ppm) δ: 1.68 (s, 3H, *o*-Mes–CH$_3$), 1.72 (s, 3H, *o*-Mes–CH$_3$), 1.96 (s, 3H, *o*-Mes–CH$_3$), 2.00 (s, 3H, *o*-Mes–CH$_3$), 2.42 (s, 3H, *p*-Mes–CH$_3$), 2.44 (s, 3H, *p*-Mes–CH$_3$), 4.07 (d, 2H, *J* = 6.6 Hz, CH═CH Juglone *trans* N), 4.07 (d, 2H, *J* = 6.6 Hz, CH═CH Juglone *trans* N), 4.26 (d, 2H, *J* = 6.6 Hz, CH═CH Juglone *trans* N), 4.50 (d, 2H, *J* = 6.6 Hz, CH═CH Juglone *trans* C), 4.51 (d, 2H, *J* = 6.6 Hz, CH═CH Juglone *trans* C), 5.04–5.21 (m, 4H, NCH$_2$), 6.77–6.78 (m, 2H, CH═CHIm), 6.84–6.88 (m, 2H, H^6 Juglone), 6.97–7.05 (m, 4H, Mes–CH), 7.07–7.08 (m, 1H, H^4 Juglone), 7.17–7.22 (m, 3H, H^5 Juglone, CH═CH Im), 7.27–7.32 (m, 1H, H^5 Juglone), 7.44–7.49 (m, 4H, Py–H^5, Py–H^3), 7.52 (dd, 1H, *J* = 7.6, 1.1 Hz, H^4 Juglone), 7.79–7.87 (m, 2H, Py–H^4), 8.51 (d, 1H, *J* = 4.4 Hz, Py–H^6), 8.62 (d, 1H, *J* = 4.4 Hz, Py–H^6), 13.04 (s, 1H, OH), 14.64 (s, 1H, OH).

^{13}C{^{1}H} NMR (75.0 MHz, CDCl$_3$, *T* = 253 K, ppm) δ: 17.7 (CH$_3$, *o*-Mes–CH$_3$), 17.8 (CH$_3$, *o*-Mes–CH$_3$), 18.3 (CH$_3$, *o*-Mesityl–CH$_3$), 18.4 (CH$_3$, *o*-Mes–CH$_3$), 21.4 (CH$_3$, *p*-Mes–CH$_3$), 21.5 (CH$_3$, *p*-Mes–CH$_3$), 55.5 (CH, NCH$_2$), 57.9 (CH, CH═CH Juglone *trans* N), 58.8 (CH, CH═CH Juglone *trans* N), 65.4 (CH, CH═CH Juglone *trans* C), 67.1 (CH, CH═CH Juglone *trans* C), 115.0 (C, C^4 Juglone), 116.0 (C, C^4 Juglone), 118.4, 119.1, 119.7 (C, C^6 Juglone), 120.0 (C, C^6 Juglone), 121.5 (CH, CH═CH Im), 121.6 (CH, CH═CH Im), 122.0 (CH, CH═CH Im), 122.1 (CH, CH═CH Im), 124.4 (CH, Py–C^3), 124.5 (CH, Py–C^3), 125.6 (CH, Py–C^5), 125.9 (CH, Py–C^5), 128.5 (overlapped CH, Mes–CH), 129.3 (CH, Mes–CH), 129.5 (CH, Mes–CH), 131.4 (CH, C^5 Juglone), 133.1 (CH, C^5 Juglone), 135.0, 135.2, 135.4, 135.5, 135.7, 138.0, 138.4, 138.6, 138.8, 139.0, 151.4 (CH, C^6 Juglone), 151.4 (CH, Py–C^6), 152.1 (CH, Py–C^6), 152.3, 159.6 (C, C^7 Juglone), 160.2 (C, C^7 Juglone), 173.6 (C, Py–C^2), 174.4 (C, Py–C^2), 183.9 (overlapped, C, NCN, C^3 Juglone), 184.4 (C, NCN), 188.9 (C, C^8 Juglone).

IR (KBr pellet, cm^{-1}): 2172 ν(CN), 1592 ν(CO).

Elemental analysis calcd (%) for $C_{28}H_{25}N_3O_3Pd$: C, 60.28, H, 4.52, N, 7.53; found: C, 59.97, H, 4.61, N, 7.79.

Stability studies in cell culture media

Complexes were dissolved in DMSO at 5 mM concentration and then diluted in cell media (DMEM/F12) obtaining a final concentration of 50 μM in the UV cuvette. Then, UV spectrum was monitored over time at *t* = 0, 1 h, 6 h and 24 h.

Cell viability assay

Four ovarian cancer cells lines (A2780, A2780*cis*, OVCAR-5 and KURAMOCHI) and one normal cell line (MRC-5) were employed and were grown in accordance with the supplier's (Sigma Aldrich) instructions. In brief, A2780, A2780*cis*, OVCAR-5 and KURAMOCHI cells were cultured in RPMI Medium 1640 (1×) + GlutaMAX™, FBS (10% v/v), P/S (1% v/v) and MRC-5 cell line was cultured with DMEM (1×) + GlutaMAX™, FBS (10% v/v), P/S (1% v/v), NEAA (1% v/v), NaPi (1% v/v). All cell lines were maintained at 37 °C in humidified atmosphere of 5% of CO$_2$. One thousand cancer cells per well and eight thousand cell per well (for MRC-5) were placed in 96 well plates and treated after 24 h with six different concen-

Open Access Article. Published on 04 December 2025. Downloaded on 12/24/2025 9:36:28 PM.
This article is licensed under a Creative Commons Attribution-NonCommercial 3.0 Unported Licence.

trations of Pd(II) complexes (0.001, 0.01, 0.1, 1, 10, 100) μM. After 96 h from the treatment cell viability was measured with a CellTiter glow assay (Promega, Madison, WI, USA; 1 : 1 dilution in PBS, 20 μL per well) with a Tecan M1000 instrument. IC_{50} values were calculated from logistical dose response curves. Averages were obtained from triplicates and error bars are standard deviations.

Evaluation of PIN1 expression

OVCAR-5 cells were cultured in RPMI supplemented with 10% FBS. Subsequently, 500 000 cells were plated in Petri dishes and treated with complex **6** (1 μM) or Juglone (10 μM) for 12 hours, including an untreated control sample. The cells were collected using a scraper, washed twice with PBS (2 × 10 mL) to remove any residual medium, and kept on ice. The samples were then lysed using an NP40-containing buffer supplemented with PhosSTOP (Roche, 4906845001), 200 μM sodium orthovanadate (Sigma-Aldrich, S6508), and 100 μM sodium fluoride (Sigma-Aldrich, S6776). Protein concentration was determined using the Bradford assay with the Bio-Rad Protein Assay Dye (Bio-Rad, 5000006) (Bradford, 1976). Samples were prepared using equal amounts of protein (15–20 μg), 5× Sample Buffer (GenScript, MB01015), and diluted to a final volume of 20 μL with ddH_2O. After heating at 100 °C for 10 minutes, the proteins were separated by SDS-PAGE (4–20% gel, GenScript, M42012) and transferred to a nitrocellulose membrane (GE Healthcare, 10600002) using the Mini-PROTEAN Tetra Vertical Electrophoresis Cell (Bio-Rad, 1658004).

After the transfer, the membranes were blocked for 1 hour at room temperature with 5% non-fat dry milk in TBST (0.1% Tween-20). First, the membranes were incubated with the primary antibody anti-Pin1 (1 : 250 in 5% non-fat dry milk in TBST, Santa Cruz, sc-46660) overnight at 4 °C. After washing, they were incubated with the secondary antibody, Goat anti-Mouse IgG (1 : 10 000 in 5% non-fat dry milk in TBST, Invitrogen, 31430), for 1 hour at room temperature and then developed. Subsequently, the membranes were reprobed with the primary antibody anti-HSP70 (1 : 10 000 in 5% non-fat dry milk in TBST, Santa Cruz, sc-24) overnight at 4 °C, followed by incubation with the same secondary antibody for 1 hour at room temperature, and then developed. Finally, protein signals were detected using LiteAblot® EXTEND Chemiluminescent Substrate (Euroclone, EMP013001) with the VWR® Imager CHEMI Premium (VWR, 730-1469P), and the images were analyzed with ImageJ software.

Conflicts of interest

There are no conflicts to declare.

Data availability

The datasets supporting this article have been uploaded as part of the supplementary information (SI). Supplementary information is available. See DOI: https://doi.org/10.1039/d5dt01792k.

CCDC 2441623–2441626 contain the supplementary crystallographic data for this paper.[78a–d]

Acknowledgements

This research was funded by Fondazione AIRC per la Ricerca sul Cancro, IG23566.

References

1 D. Hanahan and R. A. Weinberg, *Cell*, 2000, **100**, 57–70.
2 D. Hanahan and R. A. Weinberg, *Cell*, 2011, **144**, 646–674.
3 G. R. Bhat, I. Sethi, H. Q. Sadida, B. Rah, R. Mir, N. Algehainy, I. A. Albalaw, T. Masoodi, G. K. Subbaraj, F. Jamal, M. Singh, R. Kumar, M. A. Macha, S. Akil, A. S. A. Uddin, M. Haris and A. A. Bhat, *Cancer Metastasis Rev.*, 2024, **43**, 197–228.
4 Y.-C. Fu, S.-B. Liang, M. Luo and X.-P. Wang, *Cancer Cell Int.*, 2025, **25**, 103–121.
5 W. Sang, Z. Zhang, Y. Dai and X. Chen, *Chem. Soc. Rev.*, 2019, **48**, 3771–3810.
6 M. F. Sanmamed, P. Berraondo, M. E. Rodriguez-Ruiz and I. Melero, *Nat. Cancer*, 2022, **3**, 665–680.
7 S. Wu and R. Thawani, *Cancers*, 2025, **17**, 801–823.
8 M. Puzzo, M. De Santo, C. Morelli, A. Leggio and L. Pasqua, *Small Sci.*, 2024, **4**, 2400113.
9 A. Bergamo, P. J. Dyson and G. Sava, *Coord. Chem. Rev.*, 2018, **360**, 17–13.
10 G. Gasser and N. Metzel-Nolte, *Curr. Opin. Chem. Biol.*, 2012, **16**, 84–91.
11 T. Gianferrara, I. Bratsos and E. Alessio, *Dalton Trans.*, 2009, 7588–7589.
12 D. Gibson, *J. Inorg. Biochem.*, 2019, **191**, 77–84.
13 L. Markova, M. Maji, H. Kostrhunova, V. Novohradsky, J. Kasparkova, D. Gibson and V. Brabec, *J. Med. Chem.*, 2024, **67**, 9745–9758.
14 A. Sarkar, V. Novohradsky, M. Maji, T. Babu, L. Markova, H. Kostrhunova, J. Kasparkova, V. Gandin, V. Brabec and D. Gibson, *Angew. Chem., Int. Ed.*, 2023, **62**, e202310774.
15 T. Yempala, T. Babu, D. Karmakar, A. Nemirovski, M. Ishan, V. Gandin and D. Gibson, *Angew. Chem., Int. Ed.*, 2019, **58**, 18218–18223.
16 S. Alassadi, M. J. Pisa and N. J. Wheate, *Dalton Trans.*, 2022, **51**, 10835–10846.
17 D. Sahoo, P. Deb, T. Basu, S. Bardhan, S. Patra and P. K. Sukul, *Bioorg. Med. Chem.*, 2024, **112**, 117894.
18 X. Wang and Z. Guo, *Chem. Soc. Rev.*, 2013, **42**, 202–224.
19 T. Scattolin, V. A. Voloshkin, F. Visentin and S. P. Nolan, *Cell Rep. Phys. Sci.*, 2021, **2**, 100446.
20 A. R. Kapdi and I. J. S. Fairlamb, *Chem. Soc. Rev.*, 2014, **43**, 4751–4777.

Open Access Article. Published on 04 December 2025. Downloaded on 12/24/2025 9:36:28 PM.
This article is licensed under a Creative Commons Attribution-NonCommercial 3.0 Unported Licence.

21 W. A. Hermann, *Angew. Chem., Int. Ed.*, 2002, **41**, 1290–1309.
22 L. Cavallo, A. Correa, C. Costabile and H. Jacobsen, *J. Organomet. Chem.*, 2005, **690**, 5407–5413.
23 S. Díez-González and S. P. Nolan, *Coord. Chem. Rev.*, 2007, **251**, 874–883.
24 P. deFrémont, N. Marion and S. P. Nolan, *Coord. Chem. Rev.*, 2009, **253**, 862–892.
25 T. Scattolin, L. Canovese, N. Demitri, R. Gambari, I. Lampronti, C. Santo, F. Rizzolio, I. Caligiuri and F. Visentin, *Dalton Trans.*, 2018, **47**, 13616–13630.
26 R. Paprocka, M. Wiese-Szadkowska, S. Janciauskiene, T. Kosmalski, M. Kulik and A. Helmin-Basa, *Coord. Chem. Rev.*, 2022, **452**, 214307.
27 S. Ray, R. Mohan, J. K. Singh, M. K. Samantaray, M. M. Shaikh, D. Panda and P. Ghosh, *J. Am. Chem. Soc.*, 2007, **129**, 15042–15053.
28 T. Fong, C. Lok, C. Y. Chung, Y. E. Fung, P. Chow, T. P. Wan and C. Che, *Angew. Chem., Int. Ed.*, 2016, **55**, 11935–11939.
29 T. Scattolin, E. Bortolamiol, I. Caligiuri, F. Rizzolio, N. Demitri and F. Visentin, *Polyhedron*, 2020, **186**, 114607; T. Scattolin, E. Bortolamiol, F. Rizzolio, N. Demitri and F. Visentin, *Appl. Organomet. Chem.*, 2020, e5876.
30 T. Scattolin, E. Bortolamiol, F. Visentin, S. Palazzolo, I. Caligiuri, T. Perin, V. Canzonieri, N. Demitri, F. Rizzolio and A. Togni, *Chem. – Eur. J.*, 2020, **26**, 1.
31 T. Scattolin, A. Piccin, M. Mauceri, F. Rizzolio, N. Demitri, V. Canzonieri and F. Visentin, *Polyhedron*, 2021, **207**, 115381.
32 T. Scattolin, G. Andreetta, M. Mauceri, F. Rizzolio, N. Demitri, V. Canzonieri and F. Visentin, *J. Organomet. Chem.*, 2021, **952**, 122014.
33 E. Bortolamiol, M. Mauceri, R. Piccolo, E. Cavarzerani, N. Demitri, C. Donati, V. Gandin, S. Kranjc Brezar, U. Kamensek, M. Cemazar, V. Canzonieri, F. Rizzolio, F. Visentin and T. Scattolin, *J. Med. Chem.*, 2024, **67**, 14414–14431.
34 G. Tonon, M. Mauceri, E. Cavarzerani, R. Piccolo, C. Santo, N. Demitri, L. Orian, P. A. Nogara, J. B. T. Rocha, V. Canzonieri, F. Rizzolio, F. Visentin and T. Scattolin, *Dalton Trans.*, 2024, **53**, 8463–8477.
35 T. Scattolin, N. Pangerc, I. Lampronti, C. Tupini, R. Gambari, L. Marvelli, F. Rizzolio, N. Demitri, L. Canovese and F. Visentin, *J. Organomet. Chem.*, 2019, **899**, 120857.
36 S. S. Bhandarkar, J. Bromberg, C. Carrillo, P. Selvakumar, R. K. Sharma, B. N. Perry, B. Govindarajan, L. Fried, A. Sohn, K. Reddy and J. L. Arbiser, *Clin. Cancer Res.*, 2008, **14**, 5743–5748.
37 B. Díaz, K. T. Ostapoff, J. E. Toombs, J. Lo, M. Y. Bonner, A. Curatolo, V. Adsay, R. A. Brekken and J. L. Arbiser, *Oncotarget*, 2016, **7**, 51569–51580.
38 N. E. Kay, T. Sassoon, C. Secreto, S. Sinha, T. D. Shanafelt, A. K. Ghosh and J. L. Arbiser, *Leuk. Lymphoma*, 2016, **57**, 2409–2416.
39 (*a*) L. Canovese, F. Visentin, G. Chessa, P. Uguagliati and A. Dolmella, *J. Organomet. Chem.*, 2000, **601**, 1–15; (*b*) T. Scattolin, G. Moro, A. Serena, A. Guadagnin Pattaro, F. Rizzolio, V. Canzonieri, N. Demitri, E. Bortolamiol, L. M. Moretto and F. Visentin, *Appl. Organomet. Chem.*, 2021, **36**, e6629.
40 L. Canovese, F. Visentin, P. Uguagliati and B. Crociani, *J. Chem. Soc., Dalton Trans.*, 1996, 1921–1926.
41 T. Arasoglu, B. Mansuroglu, S. Derman, B. Gumus, B. Kocyigit, T. Acar and I. Kocacaliskan, *J. Agric. Food Chem.*, 2016, **64**, 7087–7094.
42 C. Majdi, V. Duvauchelle, P. Meffre and Z. Benfodda, *Biomed. Pharmacother.*, 2023, **162**, 114636.
43 S. R. D. Vardhini, *J. Recept. Signal Transduction*, 2014, **34**, 456–457.
44 A. Seetha, H. Devaraj and G. Sudhandiran, *J. Biochem. Mol. Toxicol.*, 2020, **34**, e22433.
45 J. Wang, Y. Cheng, R. Wu, D. Jiang, B. Bai, D. Tan, T. Yan, X. Sun, Q. Zhang and Z. Wu, *Int. J. Mol. Sci.*, 2016, **17**, 965–977.
46 J. Wang, D. Liu, X. Sun, B. Bai, D. Jiang and Z. Wu, *Phytochem. Lett.*, 2016, **18**, 186–192.
47 B. Gumus, T. Acar, T. Atabey, S. Derman, F. Sahin and T. Arasoglu, *J. Biotechnol.*, 2020, **316**, 35–44.
48 S. Chen, X. Wu and Z. Yu, *Front. Immunol.*, 2021, **12**, 687295.
49 F. D'Angeli, G. A. Malfa, A. Garozzo, G. Li Volti, C. Genovese, A. Stivala, D. Nicolosi, F. Attanasio, F. Bellia, S. Ronsisvalle and R. Acquaviva, *Antibiotics*, 2021, **10**, 159–176.
50 Y.-T. Tang, Y. Li, P. Chu, X.-D. Ma, Z.-Y. Tang and Z.-L. Sun, *Biomed. Pharmacother.*, 2022, **148**, 112748.
51 T. Ahmad and Y. J. Suzuki, *Antioxidants*, 2019, **8**, 91–104.
52 L. Hennig, C. Christner, M. Kipping, B. Schelbert, K. P. Rücknagel, S. Grabley, G. Küllertz and G. Fischer, *Biochemistry*, 1998, **37**, 5953–5960.
53 R. Ranganathan, K. P. Lu, T. Hunter and J. P. Noel, *Cell*, 1997, **89**, 875–886.
54 M. B. Yaffe, M. Schutkowski, M. Shen, X. Z. Zhou, P. T. Stukenberg, J. U. Rahfeld and K. P. Lu, *Science*, 1997, **278**, 1957–1960.
55 S.-H. Chao, A. L. Greenleaf and D. H. Price, *Nucleic Acids Res.*, 2001, **29**, 767–773.
56 L. Canovese, F. Visentin, G. Chessa, P. Uguagliati and A. Dolmella, *J. Organomet. Chem.*, 2000, **601**, 1–15.
57 L. Canovese, G. Chessa, C. Santo, F. Visentin and P. Uguagliati, *Organometallics*, 2002, **21**, 4342–4349.
58 L. Canovese, F. Visentin, G. Chessa, C. Levi, P. Uguagliati, A. Dolmella and G. Bandoli, *Organometallics*, 2006, **25**, 5355–5365.
59 L. Canovese, F. Visentin, C. Santo and A. Dolmella, *J. Organomet. Chem.*, 2009, **694**, 411–419.
60 L. Canovese, F. Visentin, G. Chessa, P. Uguagliati and G. Bandoli, *Organometallics*, 2000, **19**, 1461–1464.
61 L. Canovese, F. Visentin, G. Chessa, P. Uguagliati, C. Santo and A. Dolmella, *Organometallics*, 2005, **24**, 3297–3305.

Open Access Article. Published on 04 December 2025. Downloaded on 12/24/2025 9:36:28 PM.
This article is licensed under a Creative Commons Attribution-NonCommercial 3.0 Unported Licence.

62 E. Bortolamiol, E. Botter, E. Cavarzerani, M. Mauceri, N. Demitri, F. Rizzolio, F. Visentin and T. Scattolin, *Molecules*, 2024, **29**, 345–369.
63 L. Canovese, F. Visentin, C. Levi, C. Santo and V. Bertolasi, *Inorg. Chim. Acta*, 2011, **378**, 239–249.
64 X. Z. Zhou, O. Kops, A. Werner, P. J. Lu, M. Shen, G. Stoller and K. P. Lu, *Nature*, 2000, **403**, 556–561.
65 E. Campaner and A. Zannini, *Mol. Oncol.*, 2017, **11**, 1301–1313.
66 H. J. Han, H. W. Kwon, S. Y. Park and J. H. Kim, *Pathol., Res. Pract.*, 2012, **208**, 140–145.
67 J. Wang, K. Liu, X.-F. Wang and D.-J. Sun, *Oncol. Rep.*, 2017, **38**, 1959–1966.
68 L. Canovese, F. Visentin, C. Levi, C. Santo and V. Bertolasi, *Inorg. Chim. Acta*, 2012, **390**, 105–118.
69 A. Lausi, M. Polentarutti, S. Onesti, J. R. Plaisier, E. Busetto, G. Bais, L. Barba, A. Cassetta, G. Campi, D. Lamba, A. Pifferi, S. C. Mande, D. D. Sarma, S. M. Sharma and G. Paolucci, *Eur. Phys. J. Plus*, 2015, **130**, 1.
70 W. Kabsch, *Acta Crystallogr., Sect. D: Biol. Crystallogr.*, 2010, **66**, 125–132.
71 R. Evans and G. N. Murshudov, *Acta Crystallogr., Sect. D: Biol. Crystallogr.*, 2013, **69**, 1204–1214.
72 M. D. Winn, C. C. Ballard, K. D. Cowtan, E. J. Dodson, P. Emsley, P. R. Evans, R. M. Keegan, E. B. Krissinel, A. G. W. Leslie, A. McCoy, S. J. McNicholas, G. N. Murshudov, N. S. Pannu, E. A. Potterton, H. R. Powell, R. J. Read, A. Vagin and K. S. Wilson, *Acta Crystallogr., Sect. D: Biol. Crystallogr.*, 2011, **67**, 235–242.
73 G. M. Sheldrick, *Acta Crystallogr., Sect. A:Found. Adv.*, 2015, **71**, 3–8.
74 G. M. Sheldrick, *Acta Crystallogr., Sect. C:Struct. Chem.*, 2015, **71**, 3–8.
75 P. Emsley, B. Lohkamp, W. Scott and K. Cowtan, *Acta Crystallogr., Sect. D:Biol. Crystallogr.*, 2010, **66**, 486–501.
76 L. Farrugia, *J. Appl. Crystallogr.*, 2012, **45**, 849–854.
77 L. Schrodinger, *The PyMOL Molecular Graphics System*. Schrodinger, LLC, 2015. https://www.pymol.org.
78 (*a*) CCDC 2441623: Experimental Crystal Structure Determination, 2025, DOI: 10.5517/ccdc.csd.cc2myq1c; (*b*) CCDC 2441624: Experimental Crystal Structure Determination, 2025, DOI: 10.5517/ccdc.csd.cc2myq2d; (*c*) CCDC 2441625: Experimental Crystal Structure Determination, 2025, DOI: 10.5517/ccdc.csd.cc2myq3f; (*d*) CCDC 2441626: Experimental Crystal Structure Determination, 2025, DOI: 10.5517/ccdc.csd.cc2myq4g.